

Accepted Manuscript

Synthesis and biological evaluation of imidazo[1,2-*a*]pyrimidines and imidazo[1,2-*a*]pyridines as new inhibitors of the Wnt/ β -catenin signaling

Barbara Cosimelli , Sonia Laneri , Carmine Ostacolo , Antonia Sacchi , Elda Severi , Elena Porcù , Elena Rampazzo , Enrico Moro , Giuseppe Basso , Giampietro Viola



PII: S0223-5234(14)00503-0

DOI: [10.1016/j.ejmech.2014.05.071](https://doi.org/10.1016/j.ejmech.2014.05.071)

Reference: EJMECH 7029

To appear in: *European Journal of Medicinal Chemistry*

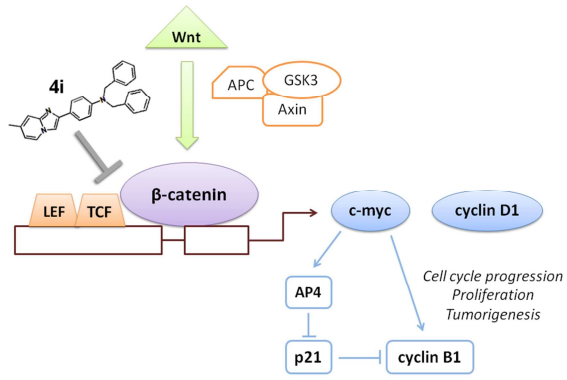
Received Date: 27 January 2014

Revised Date: 19 May 2014

Accepted Date: 30 May 2014

Please cite this article as: B. Cosimelli, S. Laneri, C. Ostacolo, A. Sacchi, E. Severi, E. Porcù, E. Rampazzo, E. Moro, G. Basso, G. Viola, Synthesis and biological evaluation of imidazo[1,2-*a*]pyrimidines and imidazo[1,2-*a*]pyridines as new inhibitors of the Wnt/ β -catenin signaling, *European Journal of Medicinal Chemistry* (2014), doi: 10.1016/j.ejmech.2014.05.071.

This is a PDF file of an unedited manuscript that has been accepted for publication. As a service to our customers we are providing this early version of the manuscript. The manuscript will undergo copyediting, typesetting, and review of the resulting proof before it is published in its final form. Please note that during the production process errors may be discovered which could affect the content, and all legal disclaimers that apply to the journal pertain.



ACCEPTED MANUSCRIPT

Synthesis and biological evaluation of imidazo[1,2-a]pyrimidines and imidazo[1,2-a]pyridines as new inhibitors of the Wnt/ β -catenin signaling

Barbara Cosimelli^{a,*}, Sonia Laneri^a, Carmine Ostacolo^a, Antonia Sacchi^a, Elda Severi^a, Elena Porcù^b, Elena Rampazzo^b, Enrico Moro^c, Giuseppe Basso^b, Giampietro Viola^{b,*}

^a *Dipartimento di Farmacia, Università di Napoli Federico II, Via D. Montesano 49, 80131 Napoli (Italy)*

^b *Dipartimento di Salute della Donna e del Bambino, Università di Padova, Via Giustiniani 3, 35128 Padova, (Italy)*

^c *Dipartimento di Scienze Biomediche, Università di Padova, Viale G. Colombo 3, 35121 Padova, (Italy)*

Corresponding authors: B. C. Phone: (+39) 081678614; Fax: (+39) 081678107. E-mail: barbara.cosimelli@unina.it. G. V. Phone: (+39) 0498211451; Fax: (+39) 0498211462. E-mail: giampietro.viola.1@unipd.it

ABSTRACT:

Wnt/ β -catenin signaling plays an important role in the regulation of embryonic development and tumorigenesis. Since its deregulation results in severe human diseases, especially cancer, the Wnt signaling pathway constitutes a promising platform for pharmacological targeting of cancer. In this study we synthesized a series of imidazo[1,2-*a*]pyrimidines and imidazo[1,2-*a*]pyridines and identified some derivatives that were able to inhibit the Wnt/ β -catenin signaling pathway in a luciferase reporter assay and cell proliferation in selected cancer cell lines, endowed with APC or β -catenin gene mutations. The most active compounds significantly downregulate the expression of Wnt target genes such as c-myc and cyclin D1. Further studies indicated that these compounds function independently of GSK-3 β activity. More importantly, *in vivo* experiments, carried out on a Wnt-reporter zebrafish model indicate, in particular for compounds **4c** and **4i** as the most active compounds, an activity comparable to that of the reference compound IWR1, suggesting their potential use not only as small molecule inhibitors of the Wnt/ β -catenin signal in Wnt driven cancers, but also in other Wnt-related diseases.

Keywords: Wnt signaling; β -catenin; signal transduction; colorectal cancer; imidazo[1,2-*a*]pyrimidines; imidazo[1,2-*a*]pyridines.

Abbreviations:

APC (Adenomatous Polyposis Coli)

CBP (Cyclic AMP response element-Binding Protein)

DAPI (4',6-diamidino-2-phenylindole)

GFP (Green Fluorescent Protein)

LEF (Lymphoid Enhancing Factor)

MTT (3-(4,5-dimethylthiazol-2-yl)-2,5-diphenyl tetrazolium bromide)

TCF (T-Cell Factor)

ACCEPTED MANUSCRIPT

1. Introduction

Wnt signaling pathway is a highly conserved system which has a crucial role in embryogenesis of all metazoan, in tissue regeneration in adult organisms and in many other processes [1], including cellular proliferation, differentiation, migration and polarity [2]. Wnt ligands are a large family of secreted, hydrophobic glycoproteins which have many receptors on a variety of cell types [3]. Three different pathways have been described as signaling cascades activated upon the binding of Wnts to the receptor: the canonical Wnt/ β -catenin pathway, the non-canonical planar cell polarity (PCP) cascade, and the Wnt/ Ca^{2+} pathway [4]. This work is focused on the best understood canonical pathway. Downstream effect of activation of this cascade is transcription of a new set of genes through the β -catenin-T cell factor (TCF) complex, which regulates cell proliferation and differentiation [5]. In canonical pathway, when Wnts are associated to their cell-surface receptor Frizzled, signal cascade is active and stable β -catenin forms a complex with TCF in the nucleus, recruiting transcriptional coactivators like cyclic AMP response element-binding protein (CBP). Such complex activates the transcription of Wnt target genes. If Wnt ligands are not associated to Frizzled, the cytoplasmic complex APC–Axin2 provides a scaffold for GSK-3 β which phosphorylates β -catenin [6]. Phosphorylation is a destabilizing process for β -catenin which is rapidly degraded through the ubiquitin-proteasome pathway. Wnts and Frizzled interaction induces Dishevelled phosphorylation which, in that form, triggers GSK-3 β inhibition [7,8]. Subsequently the balance between Axin2 and β -catenin favors the latter protein and Wnt signaling is turned on [9]. A critical role of canonical cascade has been described in regulation of stem cells, and in many tissues impairment of Wnt signaling is associated with cancer [10]. Wnt involvement in human cancer is not surprising given its fundamental role in homeostasis in adult tissue [11], and it has since been buttressed by the identification of mutations in genes coding for the Wnt pathway components Axin2, Adenomatous polyposis coli (APC), and β -catenin [12]. Indeed, loss of function of Wnt components (such as the inactivation of the APC gene) or activating mutations of β -catenin are

believed to be the critical initiating steps in malignant transformation [13]. Specific genetic hit mutations in a series of oncogenes and tumor-suppressor genes (APC, KRAS, SMAD2/4, TP53) give rise to colorectal carcinomas through a series of well-characterized histopathological changes [14]. Particularly, deregulation of canonical Wnt/ β -catenin signaling through mutations in APC was recognized to be an initiating event in colon carcinogenesis [15,16]. However, despite the presence of constitutively activating mutations in APC or β -catenin, most colorectal cancers show cellular heterogeneity when β -catenin localization is analyzed, indicating a more complex regulation of Wnt signaling [17]. Anyway, the Wnt/ β -catenin signaling pathway could be qualified as one of the promising target for innovative treatment strategies of colorectal cancer [18]. Moreover, given the fact that Wnt/ β -catenin signaling is tightly regulated at multiple cellular levels, the pathway itself offers ample targeting nodal points for cancer drug development [19]. Recently, several Wnt inhibitors were identified in high-throughput screening that target the upstream signaling of β -catenin in order to promote β -catenin degradation [20]. Although these agents efficiently inhibit Wnt signaling in normal cells and some APC-mutated colon cancer cells, they may not be effective in cells containing β -catenin mutations [21]. Despite in the last years many advances have been achieved in that field, the majority of patients relapses and the survival with metastatic disease remains approximately two years, indicating the need for new therapies that may produce dramatic improvements [22]. As just noted, high-throughput screening of synthetic compounds libraries was used to identify several Wnt inhibitors [20, 23, 24], as well as agonists [25,26]. This method efforts several structures all characterized by a pyrimidine ring decorated with a large variety of substituents or, also, condensed with other heterocycle rings (see as example compounds reported into Chart 1).

Chart 1 near here

In the past years we have been engaged in the synthesis of pyrimidines derivatives [27], imidazo[1,2-*a*]pyrimidines [28] and imidazo[1,2-*a*]pyridines [29], now we used our knowledge in the synthesis of these heterocycles to prepare a small library of 2,4,6-substituted pyrimidines and a small library of imidazo[1,2-*a*]pyrimidines and imidazo[1,2-*a*]pyridines that resemble geometry or functional groups of the known active compounds; indeed it has been reported that some NSAIDs are potential Wnt pathway therapeutics [30], and the imidazo[1,2-*a*]pyridine derivatives are often compared to indomethacin [31,32] that is active on Wnt pathway [33]. The molecules reported in Chart 2 were then evaluated for their biological activity on WNT pathway.

Chart 2 near here

2. Chemistry

The derivatives **1e** and **1f** were synthesized as previously described [27]. A similar method (Scheme 1) was performed to obtain compounds **1a-d**, and **2a-d**. Starting from the commercially available 4-amino-6-hydroxy-2-mercaptopyrimidine monohydrate (**5**), first of all was allowed the alkylation of the sulfur atom in 2-position by reaction with benzylbromide in NaOH 1M to give compound **6** [27] which was collected by filtration and resulted sufficiently pure to be used in the next step without further purification. As known [27], the second step, i.e. the alkylation of the derivative **6**, always gave, due to the keto-enol equilibrium of the pyrimidinone scaffold, a mixture of the isomeric products **1a,1c** and **2a,2c**, respectively. The experimental conditions were extensively studied with regards to solvent (DMF, acetonitrile,...), base quantities, temperature, and time of reaction. The best results were obtained when the reaction was carried out in aqueous DMF in the presence of K₂CO₃ as base and a threefold excess of haloalkane. The isomers were then easily isolated by flash-chromatography and characterized. The final step was the conversion of the amino group of **1a,1c** or **2a,2c**, into the amide group of **1b,1d** or **2b,2d** by reaction with acetyl chloride in THF.

Scheme 1 near here

The synthetic method used to prepare imidazo[1,2-*a*]pyridine and pyrimidine compounds is based on the reaction of an heteroarylamine with an α -haloacetophenone: in this case, the reaction of the opportune 2-aminopyrimidine with 4-nitrobromoacetophenone in ethanolic solution afforded (Scheme 2) the required new 5,7-disubstituted 2-(4-nitrophenyl)imidazo[1,2-*a*]pyridimidine derivative **3a** and successively the reaction with SnCl₂ in DMF of **3a** gave the required **3b**. Compound **3b** and iodomethane (ratio 2:1) in CHCl₃ and DMAP gave the desired **3c**; whereas the reaction of **3b** and benzylbromide (ratio 1:3) in the same conditions gave the required derivatives **3d** and **3e** (Scheme 2).

Scheme 2 near here

The similar compounds **3f** [34], **4a** [29], **4b** [29], **4e** [29], **4f** [35], and **4g** [35,36] have been previously reported in literature.

Benzyl bromide was allowed to react with **3f** [34], (molar ratio = 1:2) in a solution of CHCl₃ and DMAP to give the new **3g** (Scheme 3).

Scheme 3 near here

From aminopyrimidines **4b** [29], or **4g** [35,36] and benzyl bromide (molar ratio = 1:3) we obtained, in the usual conditions, the derivatives **4c** and **4d** or **4h** and **4i**, respectively (Scheme 4):

Scheme 4 near here

Finally, the amide **4j** was obtained by **4g** [35,36] and phthalic anhydride (ratio 1:2) in dioxane solution (Scheme 5):

Scheme 5 near here

3. Results and Discussion

3.1. Newly synthesized compounds impaired TCF/LEF transcriptional activity

In order to evaluate the effect of the new compounds on the Wnt/ β -catenin signaling cascade, we used a luciferase-reporter system. After liposomal transfection to insert into HT-29 cells the BAT-LUX vector, containing luciferase gene downstream the TCF/LEF promoter [37], we treated the transfected cells with our derivatives for 24 hours. Then, the cells were assayed for the β -catenin/TCF mediated activity. The data are depicted in Table 1 in which the IC_{50} values represent the concentrations that cause 50% inhibition of β -catenin transcriptional activity. Two known inhibitors of the Wnt signaling response were used as reference compounds: IWR1, an Axin stabilizer [23], and ICG001 which is endowed with an effect downstream the β -catenin degradation complex, disrupting the CBP- β -catenin interaction [38]. Pyrimidine derivatives **1a-d** and **2a-2d** were inactive or moderately active. Among the imidazo[1,2-a]pyridine derivatives compounds **4c**, **4d**, **4h** and **4i** showed a good activity, similar to that of the two reference compounds. The most active compound **4a** has a *p*-nitrophenyl while the activity decrease in **4b** where an aminophenyl is present. Interestingly, **4f**, that is the isomer of **4a**, had reduced activity pointing out that the position of methyl group has an important role in modulating the activity. On the contrary **4g**, the isomer of **4b**, have has similar efficacy.

Table 1 near here

The 5,7-dimethoxy-2-(4-nitrophenyl)imidazo[1,2-*a*]pyridimidine derivatives **3a**, **3c**, **3d** and **3e** were inactive except **3b** whereas 5-(hydroxyl)-7-methyl-2-(4-nitrophenyl)imidazo[1,2-*a*]pyrimidine (**3f**) and 5-(benzyloxy)-7-methyl-2-(4-nitrophenyl)imidazo[1,2-*a*]pyrimidine (**3g**) exhibit a value of IC₅₀ lower than both IWR1 and ICG001.

3.2. Biological *in vitro* activity: antiproliferative studies

All derivatives were tested in a panel of four human cancer cell lines to determine their antiproliferative activity after 72 hours of treatment. We used two human colon adenocarcinoma cell lines, HT-29 and LoVo, with mutated APC gene and the liver hepatocellular carcinoma HepG2 cell line, endowed with endogenously mutated β -catenin gene. In addition, the pulmonary epithelial cancer cells A549, endowed with high levels of Wnt2 were also used. All of the reported mutations result in an upregulated Wnt signaling [39,40]. As shown in Table 2, GI₅₀ values in all cell lines ranging from 5.7 to more than 100 μ M, and the more active compounds against all cell lines are **4i** and **4c** which exhibited a lower GI₅₀ values in comparison to the reference compounds IWR1 and ICG001, in the two colon adenocarcinoma cell lines (HT-29 and LoVo). Compound **4i** on HepG2 and A549 cells presented an higher activity respect to IWR1 but slightly lower than ICG001. On the other hand, **4c** was ineffective in HepG2 and was endowed with a higher value of GI₅₀ in A549 cells. Interestingly, some of the most active compounds (**3f**, **4c**, **4h**, **4i**) exhibited a lower activity or were ineffective in a primary cell line of human fibroblast, in which the Wnt/ β -catenin signaling status is inactive (Supporting Information, Table 1SI), suggesting that these compounds are selectively toxic to cell lines harboring deregulation of the Wnt/ β -catenin pathway. On the basis of the results obtained both in the luciferase-based assay and in the antiproliferative studies, we selected five molecules (**3f**, **4a**, **4c**, **4e**, **4i**), within the more active compounds that induce antiproliferative effects and antagonist action to β -catenin transcriptional activity, that were further evaluated for their ability to decrease the expression of Wnt target genes in HT-29 cell line.

Table 2 near here**3.3. β -catenin transcriptional activity was modulated independently by GSK-3 β .**

To evaluate on which step of Wnt/ β -catenin signaling these compounds act, we treated HT-29 cells transfected with BAT-LUX plasmid, with selected compounds in the presence or absence of LiCl, a GSK-3 β inhibitor. LiCl avoids β -catenin degradation by GSK-3 β enzyme, thus the effect on luciferase activity resulted independent by this enzyme. As reported in Figure 1, LiCl increased the TCF/LEF transcriptional activity by four times respect to the untreated cells, while the selected compounds, at the concentration of 25 μ M, remarkably reduced luciferin luminescence both in absence and in presence of LiCl, after 24 hours of treatment, indicating that their effect did not depend on GSK-3 β activity.

Figure 1 near here

Moreover, as shown in Figure 2, the mRNA expression of Axin2 was generally upregulated in particular by **4i** and **3f** as well as the reference compounds, confirming an inhibitory effect on Wnt pathway. In this context, it is worthwhile to note that new molecules have been described as Axin2 inducers or stabilizers [23], given its role as Wnt signaling repressor. On the other hand Axin2 itself is also a direct target of the Wnt signaling and regulates the pathways through a negative feedback loop. Its upregulation after treatment with our compounds, suggest that a repressive mechanism on Wnt pathway has been activated.

Figure 2 near here**3.4. Upstream β -catenin modulators were differently regulated by selected compounds.**

We investigated if the most active compounds alter the expression of the main molecules of the canonical Wnt pathway, that trigger β -catenin translocation into the nucleus. Immunoblot analysis depicted in Figure 3, shows that total levels of β -catenin protein were not modified after treatment. On the other hand we observed β -catenin dephosphorylation in S33/37/T41 induced by **4e**, **4i** and particularly **4c**. Interestingly, treatment with the new compounds led to modifications in β -catenin localization, mainly sited into the cytoplasm in its inactive form (shown in red, Figure 4 and Supporting Information 1SI).

Figure 3 near here

Figure 4 near here

None of the tested compounds impaired GSK-3 α/β phosphorylation in Ser21/Ser9. T-cell Factors (TCF) have essential nuclear functions, they consist in several isoforms, and the major transducers of Wnt signaling in the intestine and the oncogenic drivers of colon cancer are TCF-1 and TCF-4 [41]. It is also known that TCF-1 expression is regulated by APC and β -catenin–TCF-4 [42]. As shown in Figure 3, it appears that **3f**, **4c** and **4e** induced an increased TCF-1 protein level, but on the contrary, **4i** particularly reduced TCF-1, preventing its co-activation effect on β -catenin. Moreover, all the selected compounds remarkably reduced the mRNA expression of TCF4 (Figure 2), being the more effective compound **4i**. Altogether these effects contributed to make **4i** one of the most active compounds in the antiproliferative assay.

*3.5. **4c** and **4i** compounds negatively modulated the downstream Wnt/ β -catenin targets cyclin D1, cyclin B1 and c-myc.*

Cyclin D1 is a β -catenin direct target gene, required for G1/S transition, in cell cycle regulation, and involved in proliferation process. We investigated its regulation through Western blot analysis (Figure 3), and we observed a strong impairment in protein levels after **3f**, **4c**, and **4i**

treatment. Cyclin B1 is highly expressed in the majority of colorectal cancers [43], may promote carcinogenesis and later metastasis to lymph nodes [44]. It is essential for the transition from G2 phase to mitosis and it is linked to a high rate of cell proliferation. Also in this case a strong downregulation of cyclin B1 expression was noted by **3f**, **4c**, and **4i**. In this way, both inhibition of cyclin D1 and cyclin B1 could contribute to reduce cell growth induced by the compounds. To further evaluate the consequence of cyclins downregulation we analyzed the effect of the compounds on cell cycle in HT-29 cells. As showed in Figure 5, compound **4i** but not **3f** and **4c**, induced a significant accumulation in G1 along with a reduction of both S and G2/M phase. These results are in well agreement with the reduction of cyclin D1 and the remarkable increase of p21 (see Figure 3).

Another important gene directly transcribed by β -catenin after Wnt signaling activation is c-myc, an oncogenic transcription factor. As shown in Figure 2, mRNA expression was not significantly modified by the selected compounds. On the contrary, in Western blot (Figure 3), the c-myc protein migrated as two bands. The upper band is probably the phosphorylated and inactive form whereas the lower band is the unphosphorylated and activated form of the protein [45]. Interestingly, with **4i**, **4c** and **3f**, the lower band disappeared while the upper band remain substantially unmodified except for **4i** in which we observed a slight increase.

Figure 5 near here

3.5. **4c** and **4i** acted as WNT inhibitors *in vivo* zebrafish models.

We investigated the effects on Wnt/ β -catenin pathway also *in vivo*, using a Wnt-reporter zebrafish model, in order to explore the TCF/LEF functions [46]. These transgenic animals expressed a fluorescent reporter (GFP) under the control of Wnt-responsive promoters, and they showed high levels of signal in embryonic head and intestine. Therefore Wnt/ β -catenin signaling deregulation is easily detectable by fluorescence reduction. At 96 hours post

fertilization, zebrafish were maintained in E3 medium in which the compounds were solubilized and treated for 7 days at different concentrations, to determine the survival rate. As shown in Figure 6 (panel A) compounds **2d** and **4c** showed high toxicity in the concentration range 5-25 μ M while at 1 μ M they did not appear toxic. On the contrary, compound **4i**, showed high mortality only at the highest concentration used (25 μ M). On the basis of these results we set the concentration at which we investigated the GFP signal after 72 hours of treatment. The representative images concerning these experiments are reported in Figure 6 (panels B-C). In well agreement with Wnt inhibitory activity in BAT-LUX system **4c** and **4i** represent the most active compounds *in vivo*, and they strongly reduced the TCF/LEF transcription, in the intestinal zone. In Figure 6 (panel B), bright field images demonstrated as larvae treated with **4i** compound developed pericardial edema and dysmorphic craniofacial features. These peculiarities were described in embryos carrying null mutations in LEF1/TCF4 [47] and they are typical in cases where WNT/ β -catenin cascade is inhibited. Moreover, as reported in the magnified fluorescence images of intestine (Figure 6 panel B), **2d** reduced the expression of TCF/LEF green signal, and the intestine resulted thinner than control, and in **4i** treated, Wnt signal totally disappeared. A GFP signal quantification is depicted in Figure 6 (panel C) in which we can observe that **4i** strongly reduced the fluorescence signal comparable to that of IWR1.

Figure 6 near here

3.7. Proposed mechanism of action for compound **4i**.

4i compound was the most antiproliferative compound in tested cell lines, and it was able to inactivate c-myc. Moreover, after **4i** treatment, AP4 mRNA is strongly reduced and p21 is highly expressed, as shown in Figure 2 and Figure 3 respectively. Therefore **4i** compound inhibits Wnt/ β -catenin cascade, leading not only to cyclin D1 repression, but also to c-myc inactivation, and consequently to AP4 inhibition and p21 upregulation. This hypothesis is supported by the

findings of Jung and Hermeking [48] which reported that c-myc directly regulates the expression of AP4, a transcription factor which binds to recognition motifs located in the vicinity of the p21 promoter mediating transcriptional repression of p21 itself [49]. The resulting event is an impairment of cellular proliferation. Finally cyclin D1 and p21 stimulated cell cycle arrest in G1 and an antiproliferative effect, confirmed by S phase reduction (Figure 5).

The hypothetical molecular pathway deregulated after **4i** treatment is summarized in Figure 7.

Figure 7 near here

4. Conclusion

Among the synthesized compounds, we found that **4i** repressed Wnt signaling downstream of β -catenin and efficaciously inhibited the proliferation of selected cancer cell lines. The remarkable inhibition of our compounds on Wnt/ β -catenin targets suggests that these derivatives may downregulate Wnt signaling independently by β -catenin levels. Nevertheless Wnt target genes activation, like c-myc and cyclin D1, is severely impaired after treatment, leading to a reduced proliferation. Preliminary results have also indicated that these compounds are ineffective in normal cells suggesting that they could be selective toward cancer cells endowed with deregulation of the Wnt pathway. The Wnt-reporter zebrafish model provides an excellent experimental mean to test the ability of a compound to modulate Wnt signaling *in vivo*. The results obtained in this model clearly showed that our compounds are strongly inhibitors of the Wnt signaling, with an activity comparable to that of reference compound IWR1, suggesting that these compounds hold promise for potential use in the therapy of Wnt driven cancers but also for other Wnt related diseases. We are currently focusing on **4i** effects on colon cancer cells, by trying to outline its specific mechanism of action. Particularly we aim to understand how **4i** is able to inhibit cell proliferation and to arrest cell cycle, investigating the upstream pathway

of AP4-p21 axes. Moreover, we are studying the effects on the transcription factor TCF4, strongly downregulated by the treatment, and on its regulatory proteins.

5. Experimental Section

5.1. Chemistry

Evaporation was performed in vacuo (rotary evaporator). Analytical TLC were carried out on Merck 0.2 mm precoated silica gel aluminum sheets (60 F-254). Silica gel 60 (230-400 mesh) was used for column flash-chromatography. Melting points were determined using a Büchi apparatus B 540 and are uncorrected. Routine nuclear magnetic resonance spectra were recorded on a Varian Mercury_{plus} 400 spectrometer operating at 400 MHz for the proton and 100 MHz for the carbon in [D₆]DMSO solution. ESI-MS spectra were performed on an Applied Biosystems API 2000 instrument. All compounds showed $\geq 95\%$ purity. All starting chemicals as well as solvents were purchased by Sigma-Aldrich or CarloErba. Compounds **1e** [27], **1f** [27], **3f** [34], **4a** [29], **4b** [29], **4e** [29], **4f** [35], **4g** [35,36], and **6** [27], were synthesized as previously described. Spectroscopic data and elemental analysis results are reported in Supporting Information.

5.1.1. Synthesis of 2-(benzylthio)-6-isobutoxypyrimidin-4-amine **1a** and 6-amino-2-(benzylthio)-3-isobutylpyrimidin-4(3H)-one (**2a**)

1-Iodo-2-methylpropane (1.5 mL; 13.0 mmol) was added dropwise into a suspension of compound **6** (1.0 g; 4.3 mmol) in DMF (15 mL), H₂O (1.5 mL), and K₂CO₃ (4.3 mmol). The reaction mixture was warmed, under stirring, to reflux for 1-2 h (TLC analysis). After cooling, the solution was diluted with a mixture of ice/water (15 mL), and extracted with ethyl acetate (4x20 mL). The combined organic phases were dried on Na₂SO₄ and evaporated *in vacuo*. The

residue was purified by flash-chromatography (ethyl acetate/petroleum ether=4:1, v/v as eluent); the faster running band gave pure **1a** (57%; white crystals, mp: 88.3-89.0 °C from ethyl acetate/*n*-hexane), the slower one gave compound **2a** (12%; white crystals, mp: 161.9-162.9 °C from ethyl acetate/ *n*-hexane).

5.1.2. Synthesis of 6-(benzyloxy)-2-(benzylthio)pyrimidin-4-amine **1c** and 6-amino-3-benzyl-2-(benzylthio)pyrimidin-4(3H)-one (**2c**)

Operating as above benzylbromide gave **1c** (40%; white crystals, mp: 109.3-110.3 °C from ethyl acetate/*n*-hexane) and **2c** (11%; white crystals, mp: 163.0-164.0 °C from ethyl acetate/*n*-hexane) using ethyl acetate/petroleum ether=2:1, v/v as eluent for flash-chromatography.

5.1.3. General Procedure for the Synthesis of acetamides (**1b,d**) and (**2b,d**)

Acetyl chloride (0.02 mL, 27 mmol) was added to a solution of the appropriate amine **1a**, **1c**, **2a**, or **2c** (4 mmol) in anhydrous THF (80 mL). After stirring for 2 h, the reaction mixture was refluxed for two additional hours. After cooling at room temperature, the mixture was poured in ice/water (20 mL) treated with a saturated solution of NaHCO₃ until basic pH and finally extracted with chloroform (3x30 mL). The combined organic phases were dried on Na₂SO₄. Removal of the solvent under reduced pressure gave the crude acetamide, which was purified by chromatography. An analytical sample was obtained by crystallization.

5.1.3.1. N-[2-(Benzylthio)-6-isobutoxypyrimidin-4-yl]acetamide (**1b**). Ethyl acetate/cyclohexane=1:3, v/v as eluent; 58%; white crystals, mp: 92.0-93.2 °C from *n*-hexane.

5.1.3.2. N-[6-(Benzyloxy)-2-(benzylthio)pyrimidin-4-yl]acetamide (**1d**). Ethyl acetate/petroleum ether=4:1, v/v as eluent; 64%; white crystals, mp: 134.3-135.3 °C from *n*-hexane.

5.1.3.3. N-[2-(Benzylthio)-1-isobutyl-6-oxo-1,6-dihydropyrimidin-4-yl]acetamide (**2b**). Ethyl acetate/cyclohexane=1:3, v/v as eluent; 50%; white crystals, mp: 138.1-139.0 °C from ethyl acetate/petroleum ether.

5.1.3.4. N-[1-Benzyl-2-(benzylthio)-6-oxo-1,6-dihydropyrimidin-4-yl]acetamide (**2d**). Ethyl acetate/petroleum ether=4:1, v/v as eluent; 56%; white crystals, mp: 79.5-80.5 °C from *n*-hexane.

5.1.4. 5,7-Dimethoxy-2-(4-nitrophenyl)imidazo[1,2-a]pyrimidine (**3a**)

A solution of 4,6-dimethoxypyrimidin-2-amine (1.6 g; 10 mmol) and 2-bromo-4'-nitroacetophenone (3.7 g; 15 mmol) in 50 mL of anhydrous ethanol was stirred and refluxed for 4-6 hours. After cooling, ethanol was removed in vacuo and the residue was treated with NaHCO₃ saturated solution and extracted with CHCl₃ (3x30 mL). The combined organic phases were dried on Na₂SO₄. Removal of the solvent under reduced pressure gave the crude product which was purified by chromatography (diethyl ether/*n*-hexane=4:1, v/v as eluent, 82%). An analytical sample was obtained by crystallization from *n*-hexane (yellow crystals, mp >250 °C dec.).

5.1.5. 4-(5,7-Dimethoxyimidazo[1,2-a]pyrimidin-2-yl)aniline (**3b**)

A solution of 5,7-dimethoxy-2-(4-nitrophenyl)imidazo[1,2-a]pyridine (0.6 g; 2 mmol) and SnCl₂ (1.9 g; 10 mmol) in DMF (10 mL) was stirred and refluxed at 140°C for 4h. After cooling, NaHCO₃ saturated solution was added and the water phase was extracted with CHCl₃ (4x30 mL). The combined organic phases were dried on Na₂SO₄, concentrated *in vacuo* and then purified by chromatography (methanol/chloroform=1:9, v/v as eluent, 77%). An analytical sample was obtained by crystallization from ethyl acetate (white crystals, mp: 214.2-216.5 °C).

5.1.6. General Procedure for the Synthesis of *N*-benzyl **3d**, **4c**, **4h**, and *N,N*-dibenzyl derivatives

3e, **4d**, **4i**

The appropriate amine (4 mmol) was dissolved in anhydrous CHCl₃ (40 mL) and added of dimethylaminopyridine (0.48 g; 4 mmol) and benzyl bromide (2.05 g; 1.4 mL; 12 mmol). The mixture was stirred and heated at 60 °C for 2 h. After cooling, the mixture was filtered and added of NaOH 2N until pH=10. The organic phase was collected and the aqueous phase was extracted with CHCl₃ (3x30 mL). The combined organic phases were dried on Na₂SO₄ and evaporated *in vacuo*. The residue was purified by chromatography (chloroform as eluent); the faster running band gave pure *N,N*-dibenzyl derivative whereas the slower one gave pure *N*-benzyl derivative.

5.1.6.1. *N*-Benzyl-4-(5,7-dimethoxyimidazo[1,2-*a*]pyrimidin-2-yl)aniline (**3d**). 51%; white crystals, mp: 144.9-146.9 °C from ethyl acetate.

5.1.6.2. *N,N*-Dibenzyl-4-(5,7-dimethoxyimidazo[1,2-*a*]pyrimidin-2-yl)aniline (**3e**). 30%; white crystals, mp: 123.2-125.4 °C from ethyl acetate.

5.1.6.3. *N*-Benzyl-4-(6-methylimidazo[1,2-*a*]pyridin-2-yl)aniline (**4c**). 57%. white crystals, mp: 232.3-234.1 °C from ethyl acetate.

5.1.6.4. *N,N*-Dibenzyl-4-(6-methylimidazo[1,2-*a*]pyridin-2-yl)aniline (**4d**). 27%; white crystals, mp: 117.1-121.5 °C from ethyl acetate.

5.1.6.5. *N*-Benzyl-4-(7-methylimidazo[1,2-*a*]pyridin-2-yl)aniline (**4h**). 45%; white crystals, mp 130.2-131.6 °C from ethyl acetate.

5.1.6.6. *N,N*-Dibenzyl-4-(7-methylimidazo[1,2-a]pyridin-2-yl)aniline (**4i**). 10%; white crystals, mp 214.2-216.1 °C from ethyl acetate.

5.1.7. 4-(5,7-Dimethoxyimidazo[1,2-a]pyrimidin-2-yl)-*N*-methylaniline (**3c**)

Compound **3b** (1.8 g; 4 mmol) was dissolved in anhydrous CHCl₃ (20 mL) and added of dimethylaminopyridine (0.48 g; 4 mmol) and iodomethane (0.28 g; 0.12 mL; 2 mmol). The mixture was stirred and heated at 60 °C for 2 h. After cooling, the mixture was filtered and added of NaOH 2N until pH=10. The organic phase was collected and the aqueous phase was extracted with CHCl₃ (3x30 mL). The combined organic phases were dried on Na₂SO₄, concentrated *in vacuo* and then purified by chromatography (chloroform as eluent, 72%). An analytical sample was obtained by crystallization from ethyl acetate (white crystals, mp: 182.3-184.5 °C).

5.1.8. 5-(Benzyloxy)-7-methyl-2-(4-nitrophenyl)imidazo[1,2-a]pyrimidine (**3g**)

Operating as above compound **3f** gave **3g** (81%; yellow crystals, mp >250 °C from ethyl acetate).

5.1.9. 2-[[4-(7-Methylimidazo[1,2-a]pyridin-2-yl)phenyl]carbamoyl] benzoic acid (**4j**)

Compound **4g** (0.45 g; 2 mmol) was dissolved in dioxane (20 mL) and added of phthalic anhydride (0.59 g; 4 mmol). The mixture was stirred at room temperature for 0.5 h. The obtained solid was collected by filtration and recrystallized from ethyl acetate/methanol (46%, white crystals, mp: 231 °C dec.).

5.2 Luciferase reporter gene assay

HT-29 cells were transfected with the luciferase reporter plasmid BAT-LUX (kindly provided by Prof. Stefano Piccolo, University of Padova) which codified for LEF/TCF transcription factors.

BAT-LUX plasmid constitutes seven repeats of TCF binding element and siamois minimal promoter, cloned upstream of Luciferase gene in pGL3 backbone [50]. Cells (1.4×10^4) were transfected using HiPerFect Transfection Reagent (Qiagen, USA) with $1\mu\text{g}$ BAT-LUX construct and $1\mu\text{g}$ Renilla vector as an internal transfection control, and incubated with various concentrations of selected compounds at 37°C . After 24 h, the cells were lysed in $50\mu\text{l}$ passive lysis buffer (Promega, USA). Firefly luciferase and Renilla luciferase activity were determined using the Dual-Glo Luciferase Assay System (Promega, USA). Results are expressed as the mean of normalized ratios of firefly luciferase activity and Renilla luciferase activity measurements.

5.3. Cell proliferation assay

Human colon adenocarcinoma cell lines (HT-29 and LoVo), human liver hepatocellular carcinoma cell line (HepG2) and human lung adenocarcinoma epithelial cell line (A549) were grown in DMEM medium (Gibco, Milano, Italy), supplemented with 10% fetal bovine serum (Invitrogen, Milano, Italy) and 1% penicillin G (Gibco, Milano, Italy), streptomycin (Invitrogen, Milano, Italy) and L-glutamine (Gibco, Milano, Italy). Cells were seeded in 96-well plates (7×10^3 cells/well) and after 24h medium was removed and substituted with the drug solutions, dissolved in complete medium at scalar concentrations. Each well was incubated at 37°C in a humidified 5% CO_2 incubator for 72 h. Cell viability was assayed by the 3-(4,5-dimethylthiazol-2-yl)-2,5-diphenyl tetrazolium bromide (MTT) test, as previously described [51]. The IC_{50} was defined as the compound concentration required to inhibit cell proliferation by 50%.

5.4. Quantitative real-time RT-PCR

To quantify Axin2, TCF4, c-myc, AP4 mRNA levels we designed real-time RT-PCR assays, using GUS as reference gene. Total RNA was isolated using TRIzol (Invitrogen) from HT-29 cells treated for 24 hours with the compounds. $1\mu\text{g}$ of RNA was transcribed using the

Superscript II system (Invitrogen-Gibco) in 25 μ L final volume according to the manufacturer's instructions. Quantitative real-time PCR (qRT-PCR) was performed with 1 μ L cDNA in 20 μ L using the Sybr Green method (Invitrogen-Gibco) and analyzed on an ABI PRISM 7900HT Sequence detection system (Applied Biosystems).

The oligonucleotides to amplify mRNA fragments were Axin2 (forward 5'-CAAGGGCCAGGTCACCAA, reverse 3'-CCCCCAACCCATCTTCGT), TCF4 (forward 5'-GACGACAAGAAGGATATCAAATCA, reverse 3'-ATCCTCCGCTCCTTCTCAC), c-myc (forward 5'-AGGACCCGCTTCTCTGAAA, reverse 3'-TTCCTGTTGGTGAAGCTAACG), AP4 (forward 5'-GAGCCAGCCTGGGATTGTC, reverse 3'-GTGCTTAAAGGAGAAAGAAGAAAACC) and GUS (forward 5'-GAAAATATTGTGGTTGGAGAGC, reverse 3'-CGAGTGAAGATCCCCTTTTTTA). After normalization on GUS, expression regulation was calculated respect to untreated cells.

5.5. Western blot analysis

HT-29 cells were incubated in the presence of test compounds and, at 24 h, were collected, centrifuged, and washed twice with ice-cold PBS. Pellet was then resuspended in lysis buffer. After the cells were lysed on ice for 30 min, lysates were centrifuged at 15 000 g at 4°C for 10 min. The protein concentration in the supernatant was determined using BCA protein assay reagents (Pierce, Italy). Equal amounts of protein (10 μ g) were resolved by SDS-PAGE (12% acrylamide) and transferred to PVDF Hybond-p membrane (GE Healthcare). Membranes were blocked overnight with ECL Advance Blocking Agent (GE Healthcare), under rotation at 4 °C. Membranes were then incubated with a primary antibody against TCF-1 (rabbit, 1:1000, Cell Signaling), β -catenin (S33/37/T41) (rabbit, 1:500, Cell Signaling), β -catenin (mouse, 1:1000, Cell Signaling), GSK-3 α / β (S21/9) (rabbit, 1:1000, Cell Signaling), p21 Waf1/Cip1 (DCS60) (mouse, 1:1000, Cell Signaling), cyclin D1 (rabbit, 1:1000, Cell Signaling), c-myc (mouse, 1:200, Calbiochem), cyclin B1 (rabbit, 1:1000, Cell Signaling), or β -actin (mouse, 1:10 000, Sigma) for 1 h at room temperature. Membranes were next incubated with peroxidase-labeled goat anti-

rabbit IgG (1:100 000, Sigma) or peroxidase-labeled goat antimouse IgG (1:100 000, Sigma) for 1 h. All membranes were visualized using ECL Advance (GE Healthcare) and exposed to Amersham Hyperfilm ECL (GE Healthcare). To ensure equal protein loading, each membrane was stripped and re-probed with anti- β -actin antibody.

5.6. Immunofluorescence analysis

Cells were fixed in cold 4% formaldehyde for 15 min, rinsed and stored prior to analysis.

Primary antibody staining was performed for β -catenin (mouse, 1:50, BD Biosciences) After incubation, cells were washed and incubated with a secondary antibody conjugated to Alexa dyes (1:2000, Life technologies, Monza, Italy). Cells were counterstained with DAPI (1:10000, Sigma-Aldrich, Milano, Italy). Images were obtained on a video-confocal microscope (Vico, Eclipse Ti80, Nikon), equipped with a digital camera, using an objective 60x.

5.7. Flow cytometric analysis of cell cycle distribution

For flow cytometric analysis of DNA content, 1.5×10^5 HT-29 cells in exponential growth were treated with different concentrations of the test compounds for 24 h. After the incubation, the cells were collected, centrifuged, and fixed with ice-cold ethanol (70%). The cells were treated with lysis buffer containing RNase A and 0.1% Triton X-100 and stained with PI. Samples were analyzed on a Cytomic FC500 flow cytometer (Beckman Coulter). DNA histograms were analyzed using MultiCycl for Windows (Phoenix Flow Systems).

5.8. In vivo treatment on zebrafish model

We used wild type zebrafish, raised and maintained under standard conditions, to test our chemical compounds. Larvae were treated at 72 hours post-fertilization, until 7 days after treatment, in order to investigate compound toxicity and the survival rate. The compounds were solubilized in E3 medium, replaced every day with new medium with containing compounds.

The effect on Wnt/ β -catenin signaling was investigated using TCF/LEF-GFP reporter zebrafish. They were treated at 24 hours post-fertilization, for 72 hours. Reporter expression was visualized using the fluorescent microscope (Nikon SMZ 1500) with a GFP filter and objective 8X. 40X images were captured by a confocal microscope (Nikon A1R-A1). The quantification of fluorescence emission was carried out by ImageJ software.

ACCEPTED MANUSCRIPT

References:

- [1] A. Klaus, W. Birchmeier, Wnt signalling and its impact on development and cancer, *Nat. Rev. Canc.* 8 (2008) 387-398.
- [2] A.W. Burgess, M.C. Faux, M.J. Layton, R.G. Ramsay, Wnt signaling and colon tumorigenesis - A view from the periphery, *Exp. Cell Res.* 317 (2011) 2748-2758.
- [3] A. Kikuchi, H. Yamamoto, A. Sato, Selective activation mechanisms of Wnt signaling pathways, *Trends Cell Biol.* 19 (2009) 119-129.
- [4] H. Clevers, Wnt/ β -catenin signaling in development and disease, *Cell* 127 (2006) 469–480.
- [5] R.H. Giles, J.H. van Es, H. Clevers, Caught up in a Wnt storm: Wnt signaling in cancer, *Biochim. Biophys. Acta.* 1653 (2003) 1-24.
- [6] B.M. McCartney, I.S. Näthke, Cell regulation by the Apc protein, *Curr. Opin. Cell Biol.* 20 (2008) 186-193.
- [7] M.M. Taketo, Shutting down Wnt signal-activated cancer, *Nat. Genet.* 36 (2004) 320-322.
- [8] C. Gao, Y.G. Chen, Dishevelled: The hub of Wnt signaling, *Cell. Signal.* 22 (2010) 717-727.
- [9] R.T. Peterson, Drug discovery: Propping up a destructive regime, *Nature* 461 (2009) 599-600.
- [10] T. Reya, H. Clevers, Wnt signalling in stem cells and cancer, *Nature* 434 (2005) 843–850.
- [11] Y. Miyoshi, H. Nagase, H. Ando, A. Horii, S. Ichii, S. Nakatsuru, T. Aoki, Y. Miki, T. Mori, Y. Nakamura, Somatic mutations of the APC gene in colorectal tumors: mutation cluster region in the APC gene, *Hum. Mol. Genet.* 1 (1992) 229-233.
- [12] P. Polakis, The many ways of Wnt in cancer, *Curr. Opin. Genet. Dev.* 17 (2007) 45–51.
- [13] F. de Sousa E Melo, L. Vermeulen, D. Richel, J.P. Medema, Targeting Wnt Signaling in Colon Cancer Stem Cells, *Clin. Cancer Res.* 17 (2011) 647-653.
- [14] R. Fodde, R. Smits, H. Clevers, APC, signal transduction and genetic instability in colorectal cancer, *Nat. Rev. Canc.* 1 (2001) 55-67.
- [15] M. Bienz, H. Clevers, Linking colorectal cancer to Wnt signaling, *Cell* 103 (2000) 311-320.

- [16] H. Suzuki, D.N. Watkins, K.-W. Jair, K.E. Schuebel, S.D. Markowitz, W.D. Chen, T.P. Pretlow, B. Yang, Y. Akiyama, M. Van Engeland, M. Toyota, T. Tokino, Y. Hinoda, K. Imai, J.G. Herman, S.B. Baylin, Epigenetic inactivation of *SFRP* genes allows constitutive WNT signaling in colorectal cancer, *Nat. Genet.* 36 (2004) 417-422.
- [17] L. Vermeulen, F. De Sousa E Melo, F. Melo, M. van der Heijden, K. Cameron, J.H. de Jong, T. Borovski, J.B. Tuynman, M. Todaro, C. Merz, H. Rodermond, M.R. Sprick, K. Kemper, D.J. Richel, G. Stassi, J.P. Medema, Wnt activity defines colon cancer stem cells and is regulated by the microenvironment, *Nat. Cell Biol.* 12 (2010) 468-476.
- [18] B.E. Shan, M.X. Wang, R.Q. Li, Quercetin Inhibit Human SW480 Colon Cancer Growth in Association with Inhibition of Cyclin D₁ and Survivin Expression through Wnt/ β -Catenin Signaling Pathway, *Cancer Invest.* 27 (2009) 604-612.
- [19] H.H. Luu, R. Zhang, R.C. Haydon, E. Rayburn, Q. Kang, W. Si, J.K. Park, H. Wang, Y. Peng, W. Jiang, T.C. He, Wnt/ β -catenin signaling pathway as novel cancer drug targets, *Curr. Cancer Drug Targets* 4 (2004) 653-671.
- [20] S.-M.A. Huang, Y.M. Mishina, S. Liu, A. Cheung, F. Stegmeier, G.A. Michaud, O. Charlat, E. Wiellette, Y. Zhang, S. Wiessner, M. Hild, X. Shi, C.J. Wilson, C. Mickanin, V. Myer, A. Fazal, R. Tomlinson, F. Serluca, W. Shao, H. Cheng, M. Shultz, C. Rau, M. Schirle, J. Schlegl, S. Ghidelli, S. Fawell, C. Lu, D. Curtis, M.W. Kirschner, C. Lengauer, P.M. Finan, J.A. Tallarico, T. Bouwmeester, J.A. Porter, A. Bauer, F. Cong, Tankyrase inhibition stabilizes axin and antagonizes Wnt signalling, *Nature* 461 (2009) 614-620.
- [21] W. Zhang, V. Sviripa, L.M. Kril, X. Chen, T. Yu, J. Shi, P. Rychahou, B. M. Evers, D.S. Watt, C. Liu, Fluorinated *N,N*-dialkylaminostilbenes for Wnt pathway inhibition and colon cancer repression, *J. Med. Chem.* 54 (2011) 1288-1297.
- [22] W. Chen, M. Chen, L.S. Barak, Development of small molecules targeting the Wnt pathway for the treatment of colon cancer: a high-throughput screening approach, *Am. J. Physiol. Gastrointest. Liver Physiol.* 299 (2010) G293-G300.

- [23] B. Chen, M.E. Dodge, W. Tang, J. Lu, Z. Ma, C.-W. Fan, S. Wei, W. Hao, J. Kilgore, N.S. Williams, M.G. Roth, J.F. Amatruda, C. Chen, L. Lum, Small molecule-mediated disruption of Wnt-dependent signaling in tissue regeneration and cancer, *Nat. Chem. Biol.* 5 (2009) 100-107.
- [24] K. Ewan, B. Pająk, M. Stubbs, H. Todd, O. Barbeau, C. Quevedo, H. Botfield, R. Young, R. Ruddle, L. Samuel, A. Battersby, F. Raynaud, N. Allen, S. Wilson, B. Latinkic, P. Workman, E. McDonald, J. Blagg, W. Aherne, T. Dale, A Useful Approach to Identify Novel Small-Molecule Inhibitors of Wnt-Dependent Transcription, *Cancer Res.* 70, (2010) 5963-5973.
- [25] J. Liu, X. Wu, B. Mitchell, C. Kintner, S. Ding, P.G. Schultz, A small-molecule agonist of the Wnt signaling pathway, *Angew. Chem. Int. Ed.* 44 (2005) 1987–1990.
- [26] J.C. Pelletier, J.T. Lundquist IV, A.M. Gilbert, N. Alon, F.J. Bex, B.M. Bhat, M.G. Bursavich, V.E. Coleburn, L.A. Felix, D.M. Green, P. Green, D.B. Hauze, Y.P. Kharode, H.-S. Lam, S.R. Lockhead, R.L. Magolda, J.J. Matteo, J.F. Mehlmann, C. Milligan, R.J. Murrills, J. Pirrello, S. Selim, M.C. Sharp, R.J. Unwalla, M.D. Vera, J.E. Wrobel, P. Yaworsky, P.V.N. Bodine, (1- (4-(Naphthalen-2-yl)pyrimidin-2-yl)piperidin-4-yl) methanamine: A Wingless β -Catenin Agonist That Increases Bone Formation Rate, *J. Med. Chem.* 52 (2009) 6962-6965.
- [27] B. Cosimelli, G. Greco, M. Ehlaro, E. Novellino, F. Da Settimo, S. Taliani, C. La Motta, M. Bellandi, T. Tuccinardi, A. Martinelli; O. Ciampi, M.L. Trincavelli, C. Martini, Derivatives of 4-Amino-6-hydroxy-2-mercaptopyrimidine as Novel, Potent, and Selective A₃ Adenosine Receptor Antagonists, *J. Med. Chem.* 51 (2008) 1764-1770.
- [28] S. Laneri, A. Sacchi, E. Abignente, Research on heterocyclic compounds. Part XLII. The Vilsmeier reaction in the synthesis of imidazo[1,2-a]pyrimidine derivatives, *J. Heterocycl. Chem.* 37 (2000) 1265-1267.
- [29] S. Laneri, C. Di Ronza, A. Bernardi, C. Ostacolo, A. Sacchi, C. Cervone, M. D'Amico, C. Di Filippo, M.L. Trincavelli, A. Panighini, C. Martini, Synthesis and antihypertensive action of new imidazo[1,2-a]pyridine derivatives, non peptidic angiotensin II receptor antagonists, *Cardiovascular & Haematological Disorders-Drug Targets* 11 (2011) 87-96.

- [30] N. Barker, H. Clevers, Mining the Wnt pathway for cancer therapeutics, *Nat. Rev. Drug Disc.* 5 (2006) 997-1014.
- [31] Y.K. Marquez-Flores, Ma.E. Campos-Aldrete, H. Salgado-Zamora, J. Correa-Basurto, Ma.E. Melendez-Camargo, Docking simulations, synthesis, and anti-inflammatory activity evaluation of 2-(alkylamino)amino-3-(nitro)imidazo[1,2-a]pyridines, *Med. Chem. Res.* 21 (2012) 775-782.
- [32] Y.K. Marquez-Flores, Ma.E. Campos-Aldrete, H. Salgado-Zamora, J. Correa-Basurto, Ma.E. Melendez-Camargo, Acute and chronic anti-inflammatory evaluation of imidazo[1,2-a]pyridine carboxylic acid derivatives and docking analysis, *Med. Chem. Res.* 21 (2012) 3491-3498.
- [33] S. Dihlmann, S. Klein, M. von Knebel Doeberitz, Reduction of β -catenin/T-cell transcription factor signaling by aspirin and indomethacin is caused by an increased stabilization of phosphorylated β -catenin, *Mol. Cancer Ther.* 2 (2003) 509–516.
- [34] T. Pyl, W. Baufeld, Bicyclic heterocyclic compounds with a common nitrogen atom. XI. Nucleophilic substitutions of 5-chloro-7-methyl-2-phenylimidazo[1,2-a]pyrimidines, *J. Lieb. Ann. Chem.* 699 (1966) 112-126.
- [35] R.J. Sundberg, D.J. Dahlhausen, G. Manikumar, B. Mavunkel, A. Biswas, V. Srinivasan, F. King Jr., P. Waid, Preparation of 2-aryl- and 2-(aryloxymethyl)imidazo[1,2-a]pyridines and related compounds, *J. Heterocyclic Chem.* 25 (1988) 129-137.
- [36] T. Takaya, H. Takasugi, Imidazo-heterocyclic compounds, and pharmaceutical composition comprising them, *Eur. Pat. Appl.* (1984) EPXXDV EP 120589.
- [37] E. Rampazzo, L. Persano, F. Pistollato, E. Moro, C. Frasson, P. Porazzi, A. Della Puppa, S. Bresolin, G. Battilana, S. Indraccolo, G. Te Kronnie, F. Argenton, N. Tiso, G. Basso, Wnt activation promotes neuronal differentiation of Glioblastoma, *Cell Death Dis.* 4 (2013) e597 (e500).
- [38] Emami KH, Nguyen C, Ma H, Kim DH, Jeong KW, Eguchi M, Moon RT, Teo JL, Kim HY, Moon SH, Ha JR, Kahn M. A small molecule inhibitor of beta-catenin/CREB-binding protein transcription. *Proc. Natl. Acad. Sci.* 2004, 101(34), 12682-12687.

- [39] J. Li, Y. Mizukami, X. Zhang, W.-S. Jo, D.C. Chung, Oncogenic K-ras stimulates Wnt signaling in colon cancer through inhibition of GSK-3 β , *Gastroenterology* 128 (2005) 1907-1918.
- [40] E.C. Pacheco-Pinedo, A.C. Durham, K.M. Stewart, A.M. Goss, M.M. Lu, F.J. DeMayo, E.E. Morrisey, Wnt / β -catenin signaling accelerates mouse lung tumorigenesis by imposing an embryonic distal progenitor phenotype on lung epithelium, *J Clin Invest.* 121 (2011) 1935–1945.
- [41] A. Gregorieff, H. Clevers, Wnt signaling in the intestinal epithelium: From endoderm to cancer, *Genes Dev.* 19 (2005) 877-890.
- [42] J. Roose, G. Huls, M. van Beest, P. Moerer, K. van der Horn, R. Goldschmeding, T. Logtenberg, H. Clevers, Synergy between tumor suppressor APC and the β -catenin-Tcf4 target Tcf1, *Science* 285 (1999) 1923-1926.
- [43] A. Wang, N. Yoshimi, N. Ino, T. Tanaka, H. Mori, Overexpression of cyclin B1 in human colorectal cancers, *J Cancer Res Clin Oncol.* 123 (1997) 124-127.
- [44] J.Q. Li, A. Kubo, F. Wu, H. Usuki, J. Fujita, S. Bandoh, T. Masaki, K. Saoo, H. Takeuchi, S. Kobayashi, K. Imaida, H. Maeta, T. Ishida, S. Kuriyama. Cyclin B1, unlike cyclin G1, increases significantly during colorectal carcinogenesis and during later metastasis to lymph nodes, *Int J Oncol.* 22 (2003) 1101-1110.
- [45] L Tao, PM Kramer, W Wang, S Yang, RA Lubet, VE Steele, MA Pereira. Altered expression of c-myc, p16 and p27 in rat colon tumors and its reversal by short-term treatment with chemopreventive agents. *Carcinogenesis.* 23 (2002) 1447-54.
- [46] E. Moro, G. Ozhan-Kizil, A. Mongera, D. Beis, C. Wierzbicki, R.M. Young, D. Bournele, A. Domenichini, L.E. Valdivia, L. Lum, C. Chen, J.F. Amatruda, N. Tiso, G. Weidinger, F. Argenton, *In vivo* Wnt signaling tracing through a transgenic biosensor fish reveals novel activity domains, *Dev Biol.* 366 (2012) 327-340.
- [47] R.R. Doshi, A.S. Patil, A role of genes in craniofacial growth, *IIOAB J.* 3 (2012) 19-36.
- [48] P. Jung, H. Hermeking, The c-MYC-AP4-p21 cascade, *Cell Cycle* 8 (2009) 982-989.

[49]P. Jung, A. Menssen, D. Mayr, H. Hermeking, AP4 encodes a c-MYC-inducible repressor of p21, Proc. Natl. Acad. Sci. USA 105 (2008) 15046-15051.

[50]X. Wang, D. Kopinke, J. Lin, A.D. McPherson, R.N. Duncan, H. Otsuna, E. Moro, K. Hoshijima, D.J. Grunwald, F. Argenton, C.B. Chien, L.C. Murtaugh, R.I. Dorsky, Wnt Signaling Regulates Postembryonic Hypothalamic Progenitor Differentiation, Dev Cell, 23 (2012) 624-636.

[51]R. Romagnoli, P.G. Baraldi, M.K. Salvador, D. Preti, M.A. Tabrizi, A. Brancale, X.H. Fu, J. Li, S.Z. Zhang, E. Hamel, R. Bortolozzi, E. Porcù, G. Basso, G. Viola, Discovery and optimization of a series of 2-aryl-4-amino-5-(3',4',5'-trimethoxybenzoyl)thiazoles as novel anticancer agents, J Med Chem. 55 (2012) 5433-5445.

ACCEPTED MANUSCRIPT

Schemes and Figures Captions:

Scheme 1. Synthesis of pyrimidine derivatives **1a-2d**.

Scheme 2. Synthesis of compounds **3a-3e**.

Scheme 3. Synthesis of compound **3g**.

Scheme 4. Synthesis of compounds **4c, 4d, 4h, 4i**.

Scheme 5. Synthesis of compound **4j**.

Figure 1. Effect on TCF/LEF transcriptional activity in BAT-LUX system after 24 hours of treatment with **4e, 4i, 4a, 3f, 4c** compounds, at the concentration of 25 μ M alone or in combination with the GSK-3 inhibitor, LiCl (25 mM). Relative Luminescence Unit (RLU) indicates the relative intensity of luciferine signal. Data are expressed as mean \pm SEM of three independent experiments.

Figure 2. Fold changes of mRNA expression of Axin2, TCF4, c-myc, AP4. Cells were treated with indicated compounds at the concentration of 25 μ M, as well as the two reference compounds IWR1 and ICG001. After 24 hours total RNA was extracted and transcribed as described in the experimental section. Quantitative real-time PCR was then performed and the results were calibrated to untreated cells mRNA (RQ = 1), used as control.

Figure 3. Effects of **4e, 4i, 4a, 3f, 4c** on the main molecules implicated in Wnt/ β -catenin cascade. HT-29 cells were treated with the indicated compounds at 25 μ M concentration for 24

hours, harvested and lysed for Western blot analysis. To confirm equal protein loading, each membrane was stripped and reprobed with anti- β -actin antibody.

Figure 4. Representative images of HT-29 cells treated with the indicated compounds at 25 μ M for 24 hours. Immunostaining was performed for β -catenin (red), and with DAPI to stain the nuclei (blue). Pictures were acquired by fluorescent microscope using a 60X objective (Bar=100 μ m).

Figure 5. Cell cycle analysis after 24 hours of treatment with the indicated compounds at the concentration of 25 μ M in HT-29. Significant effects were detectable for **4i** compound which arrested cell cycle in G1 and decreased S phase. Data are expressed as mean \pm SEM of three independent experiments. * p <0.01 vs control cells.

Figure 6. Panel A: survival curves of zebrafish larvae treated for 7 days starting at 72 hours post-fertilization. Panel B: representative images of Wnt-reporter zebrafish treated with IWR1 and **4i** at 10 μ M, **2d** and **4c** at 1 μ M for 72 hours, starting at 24 hours after fertilization. On the left side, bright field images, merged with GFP signal, were reported. The white rectangles indicate the portions reported on the right side, representing the intestinal zone. In control larvae TCF/LEF-GFP signal, characterizing the intestine, is wide and strewn, while treated zebrafish by **2d** showed a thinner intestine. After **4i** treatment the reporter signal totally disappeared, and the fish phenotype was characterized by pericardial edema (indicated by the arrow), and craniofacial dysmorphism. Panel C: the graph summarized the fluorescence intensity measured in the intestinal zone, after compounds treatment. Data represented as mean \pm SEM of three independent experiments.

Figure 7. Schematic representation of Wnt signaling pathway and its downstream molecules probably involved in response to **4i** treatment. β -catenin target genes are downregulated after **4i** treatment, independently to GSK-3 action. c-myc deregulation leads to p21 upregulation and cyclin B1 reduction, resulting in cell cycle arrest and inhibited proliferation.

ACCEPTED MANUSCRIPT

Table 1. Wnt inhibitory effect in BAT-LUX system into HT-29 cells, of the newly investigated compounds.

Compound	IC ₅₀ (μM) ^a	Compound	IC ₅₀ (μM) ^a
1a	72.2 ± 0.7	3e	67.0 ± 3.1
1b	> 100	3f	10.4 ± 0.02
1c	> 100	3g	16.1 ± 0.01
1d	46.2 ± 1.2	4a	6.2 ± 0.003
1e	22.3 ± 0.2	4b	52.6 ± 2.3
1f	81.8 ± 2.1	4c	11.1 ± 0.005
2a	30.7 ± 1.5	4d	19.5 ± 0.03
2b	43.0 ± 0.5	4e	9.7 ± 0.007
2c	54.3 ± 1.1	4f	23.1 ± 0.03
2d	35.6 ± 0.6	4g	42.2 ± 3.2
3a	57.8 ± 2.3	4h	17.8 ± 0.1
3b	14.3 ± 0.04	4i	24.1 ± 0.02
3c	72.2 ± 3.5	4j	> 100
3d	34.6 ± 0.04	IWR1	24.4 ± 0.6
		ICG001	18.7 ± 0.3

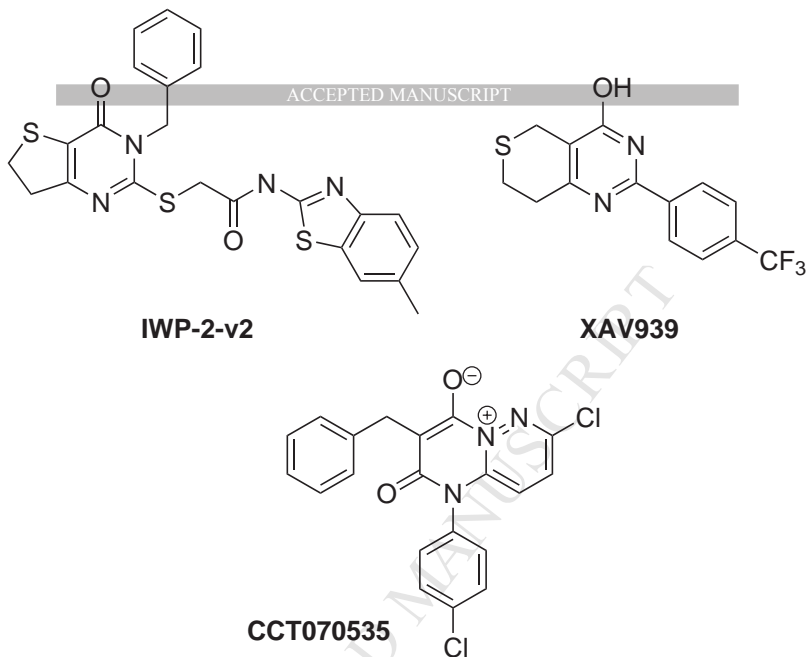
^a IC₅₀ values represent the concentration necessary to inhibit TCF/LEF transcriptional activity by 50%.

Table 2. *In vitro* cell growth inhibition after 72 hours treatment of the newly investigated compounds.

Compound	GI ₅₀ (μM) ^a			
	HT-29	LoVo	HepG2	A549
1a	40.0 ± 24.7	54.5 ± 4.9	60.8 ± 2.5	18.7 ± 12.6
1b	35.7 ± 11.7	53.9 ± 7.2	64.4 ± 3.4	19.9 ± 12.7
1c	53.9 ± 7.1	53.7 ± 3.8	49.0 ± 7.0	46.2 ± 3.9
1d	65.8 ± 1.5	40.0 ± 2.1	42.9 ± 22.1	35.2 ± 19.5
1e	88.2 ± 2.9	54.2 ± 13.2	87.1 ± 6.3	51.0 ± 29.4
1f	59.9 ± 7.9	54.9 ± 8.8	75.1 ± 3.8	75.7 ± 3.6
2a	> 100	68.0 ± 2.5	77.0 ± 11.9	83.3 ± 9.1
2b	68.4 ± 9.4	58.5 ± 5.2	67.6 ± 19.9	46.4 ± 19.2
2c	> 100	84.9 ± 15.1	97.8 ± 1.9	> 100
2d	79.3 ± 4.8	56.3 ± 6.1	71.7 ± 9.1	50.4 ± 9.0
3a	> 100	70.6 ± 29.4	35.9 ± 27.0	36.6 ± 7.6
3b	> 100	> 100	> 100	> 100
3c	> 100	> 100	> 100	> 100
3d	> 100	> 100	> 100	> 100
3e	> 100	61.9 ± 16.5	> 100	7.0 ± 1.0
3f	90.1 ± 5.0	87.6 ± 6.0	> 100	38.9 ± 12.0
3g	> 100	74.9 ± 10.6	> 100	71.0 ± 3.8
4a	> 100	> 100	> 100	> 100
4b	82.9 ± 9.0	65.2 ± 2.0	> 100	> 100
4c	8.8 ± 0.4	42.6 ± 3.5	> 100	56.1 ± 11.2
4d	37.6 ± 4.0	n.d.	n.d.	60.0 ± 6.1
4e	> 100	90.7 ± 9.3	> 100	> 100
4f	> 100	n.d.	n.d.	62.4 ± 6.5
4g	93.6 ± 5.2	n.d.	n.d.	> 100
4h	17.5 ± 2.6	n.d.	n.d.	5.1 ± 0.7
4i	6.9 ± 1.2	5.7 ± 0.5	18.4 ± 10.0	17.2 ± 6.9
4j	> 100	n.d.	n.d.	> 100
IWR1	> 100	63.1 ± 7.7	95.4 ± 4.5	> 100
ICG001	17.2 ± 2.9	15.6 ± 2.8	12.7 ± 1.5	6.1 ± 0.1

[a] GI₅₀ indicates the required concentration to inhibit tumor cell proliferation by 50%. Data are expressed as the mean ± SEM from the dose–response curves of at least three independent experiments. n.d. not determined

Inhibitors from high-throughput screening:



Inhibitors as reference compounds:

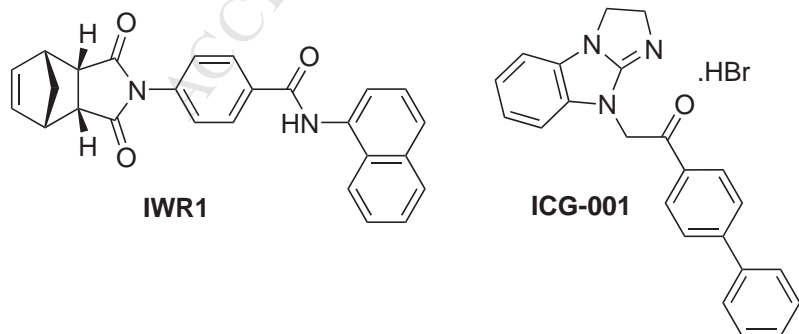
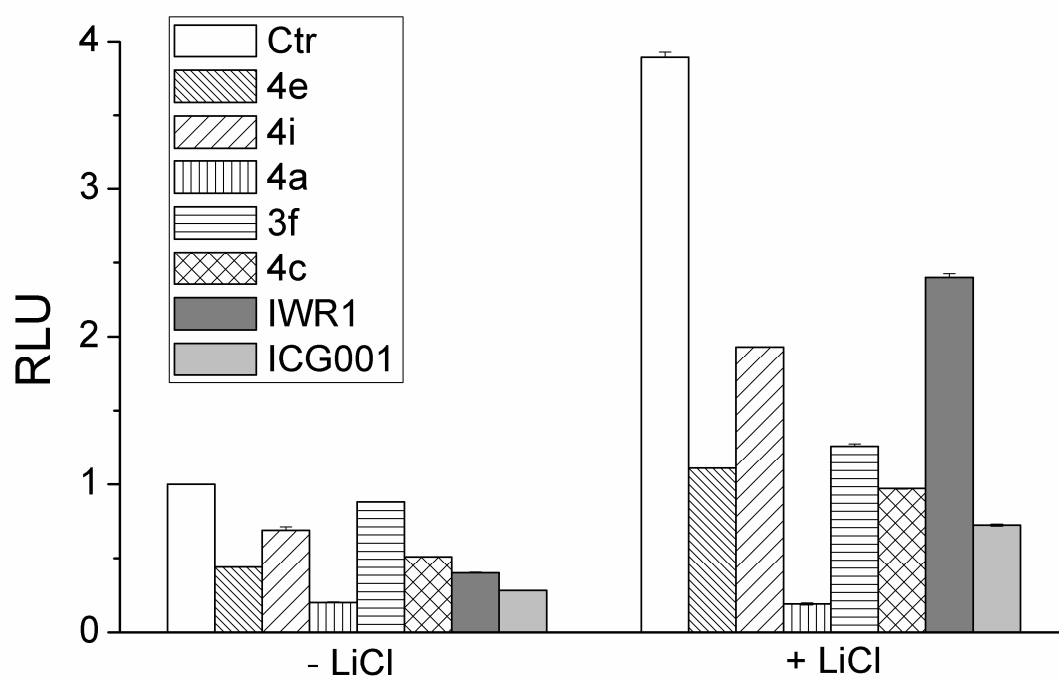
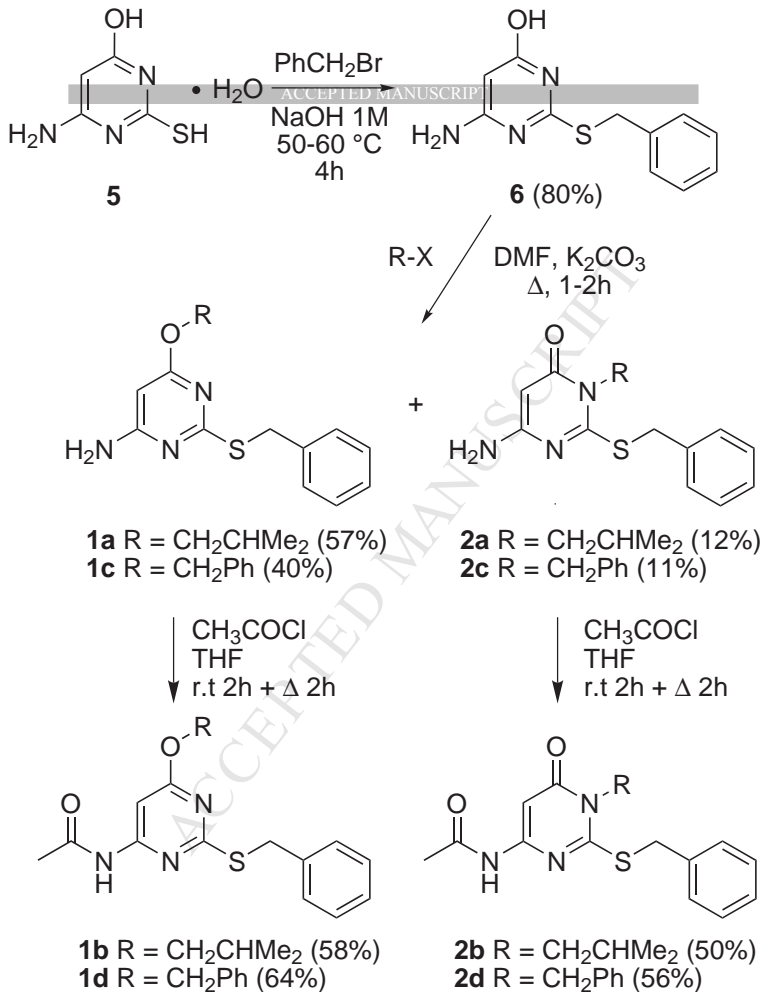


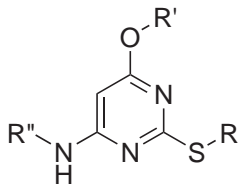
Figure 1



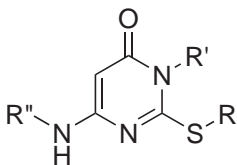
ACCEPTED MANUSCRIPT



Scheme 1

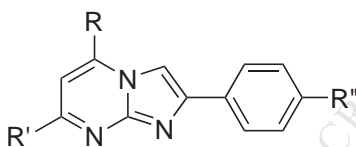


1a-f

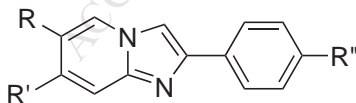


2a-d

- 1a,2a** R = CH₂Ph; R' = CH₂CHMe₂; R'' = H
1b,2b R = CH₂Ph; R' = CH₂CHMe₂; R'' = COMe
1c,2c R = R' = CH₂Ph; R'' = H
1d,2d R = R' = CH₂Ph; R'' = COMe
1e R = CH₂CH₂Me; R' = CH₂Ph, R'' = H
1f R = CH₂CH₂Me; R' = CH₂Ph, R'' = COMe

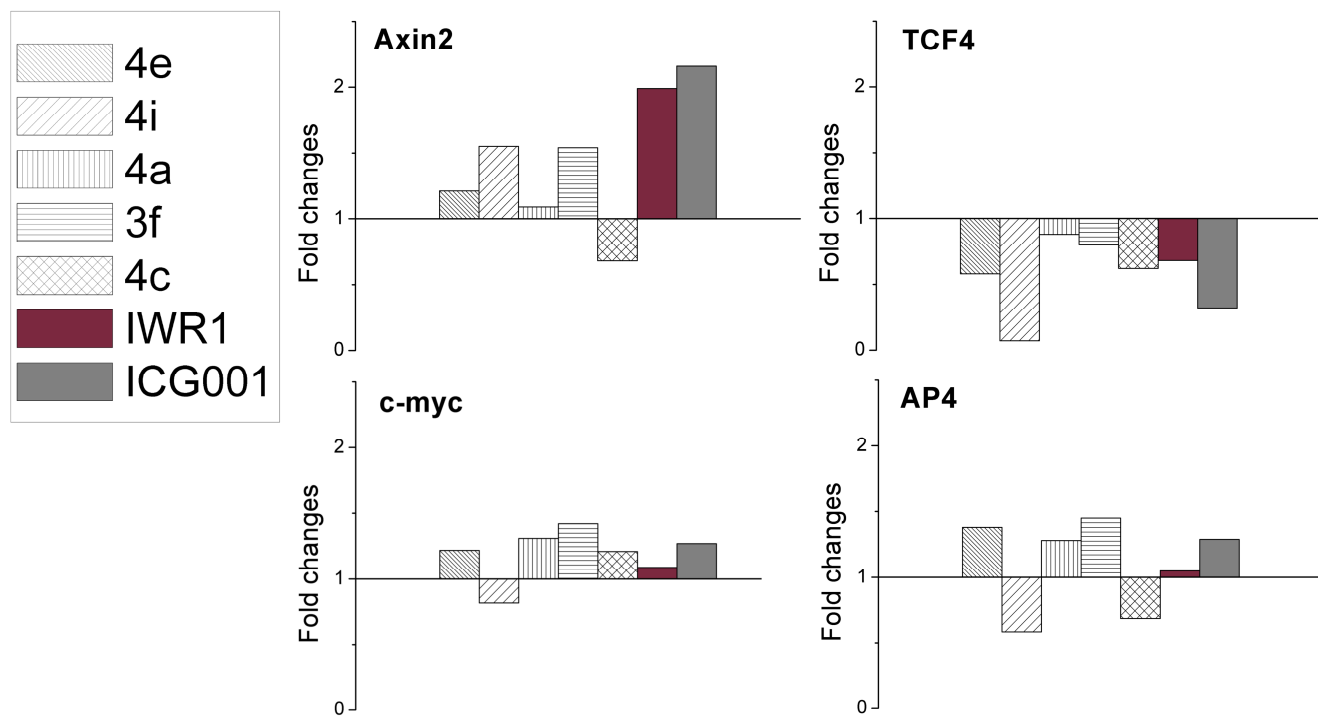


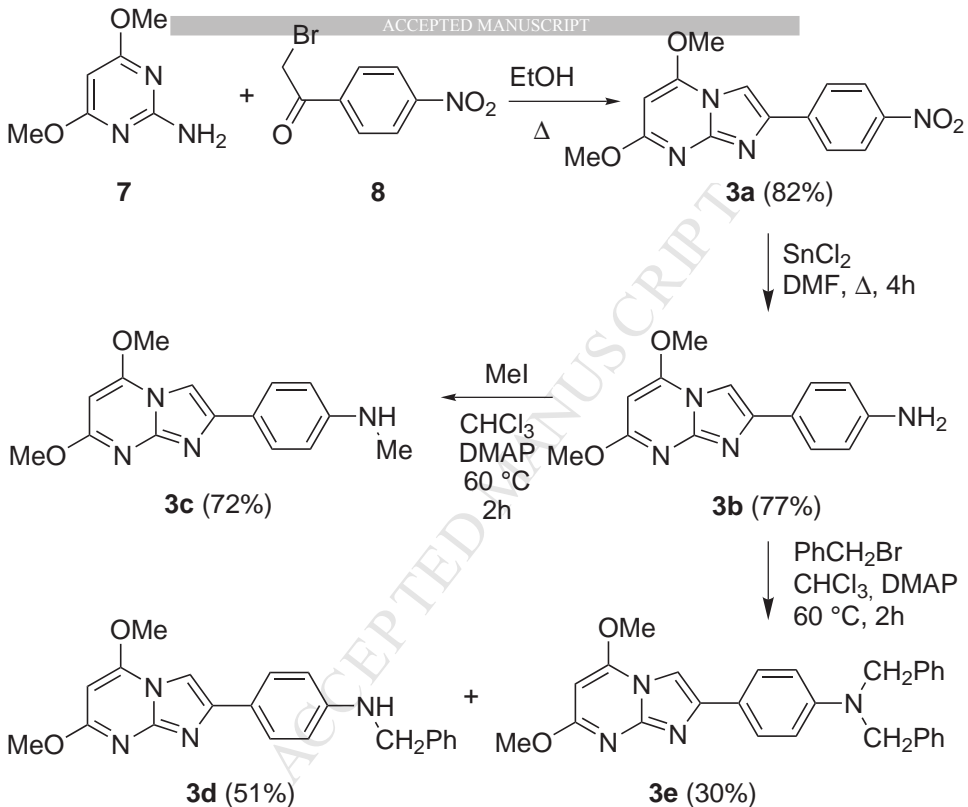
- 3a** R = R' = OMe; R'' = NO₂
3b R = R' = OMe; R'' = NH₂
3c R = R' = OMe; R'' = NHMe
3d R = R' = OMe; R'' = NHCH₂Ph
3e R = R' = OMe; R'' = N(CH₂Ph)₂
3f R = OH; R' = Me; R'' = NO₂
3g R = OCH₂Ph; R' = Me; R'' = NO₂



- 4a** R = Me; R' = H; R'' = NO₂
4b R = Me; R' = H; R'' = NH₂
4c R = Me; R' = H; R'' = NHCH₂Ph
4d R = Me; R' = H; R'' = N(CH₂Ph)₂
4e R = Me; R' = H; R'' = NHCO(C₆H₄)COOH-o
4f R = H; R' = Me; R'' = NO₂
4g R = H; R' = Me; R'' = NH₂
4h R = H; R' = Me; R'' = NHCH₂Ph
4i R = H; R' = Me; R'' = N(CH₂Ph)₂
4j R = H; R' = Me; R'' = NHCO(C₆H₄)COOH-o

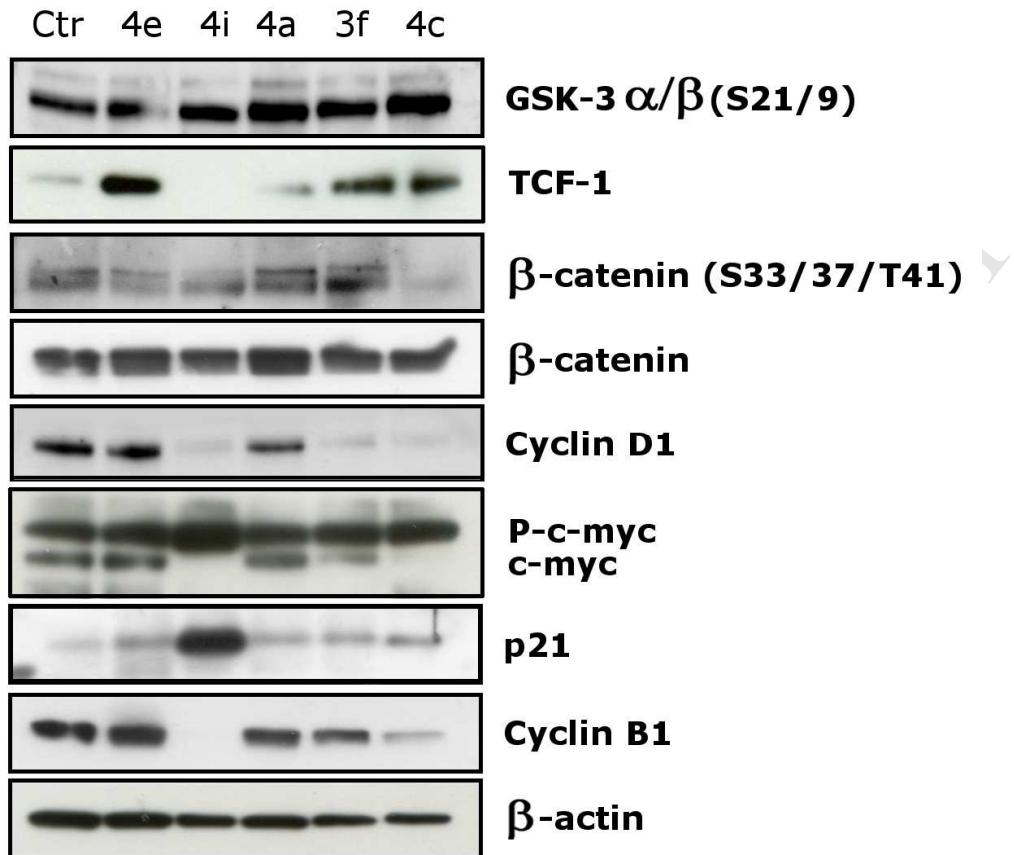
Figure 2.



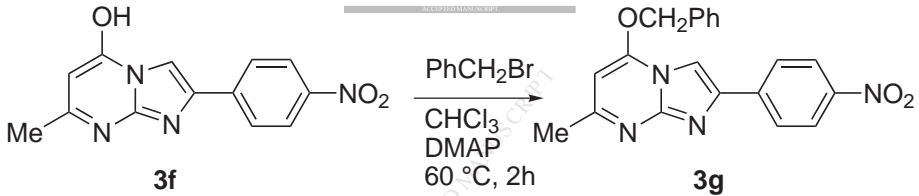


Scheme 2

Figure 3.

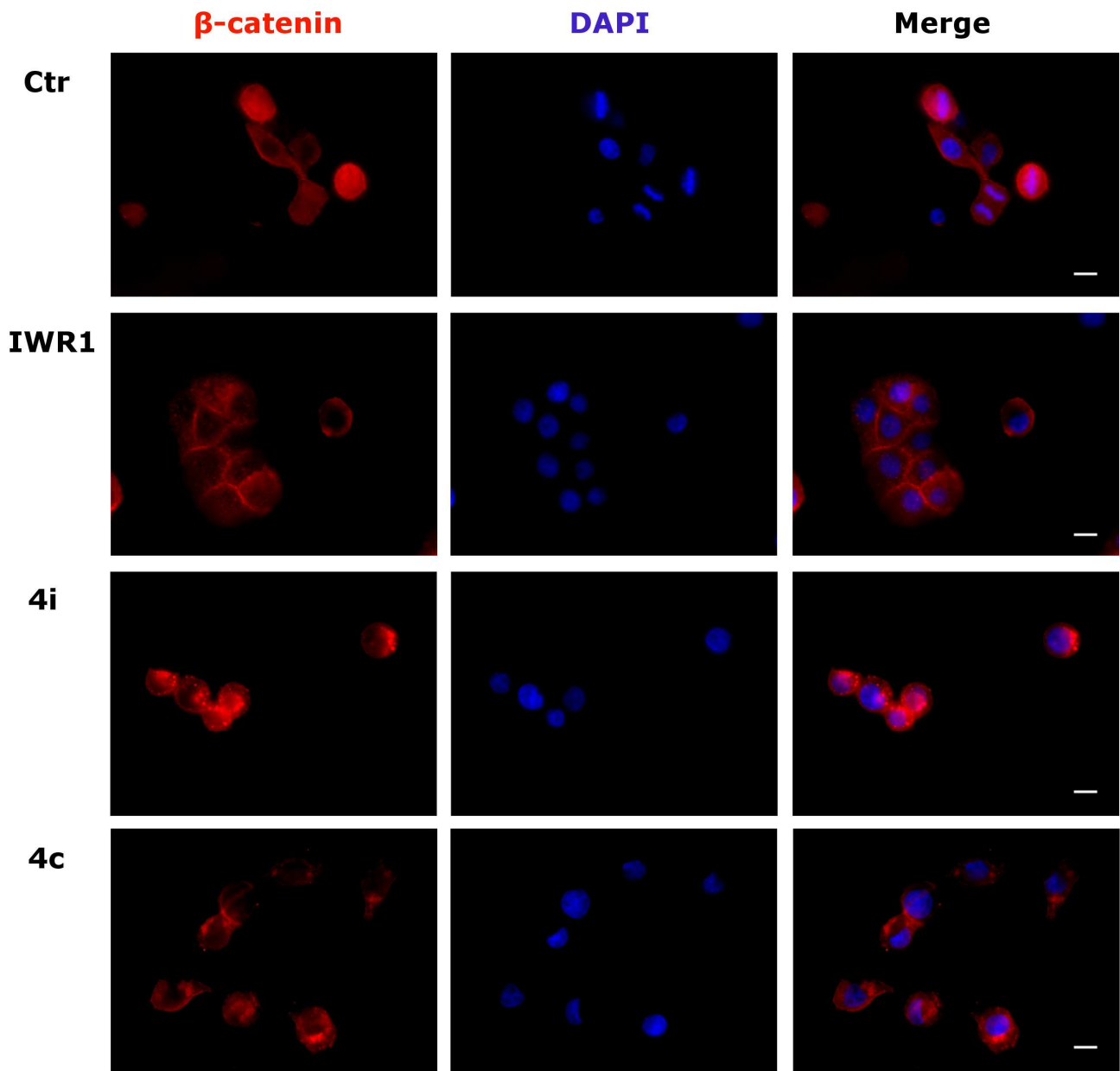


ACCEPTED

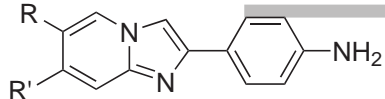


Scheme 3

Figure 4.

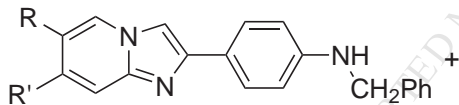
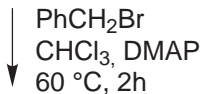


ACC



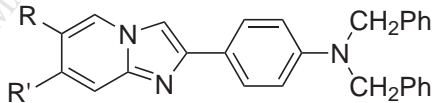
4b R = Me; R' = H

4g R = H; R' = Me



4c R = Me; R' = H (57%)

4h R = H; R' = Me (45%)

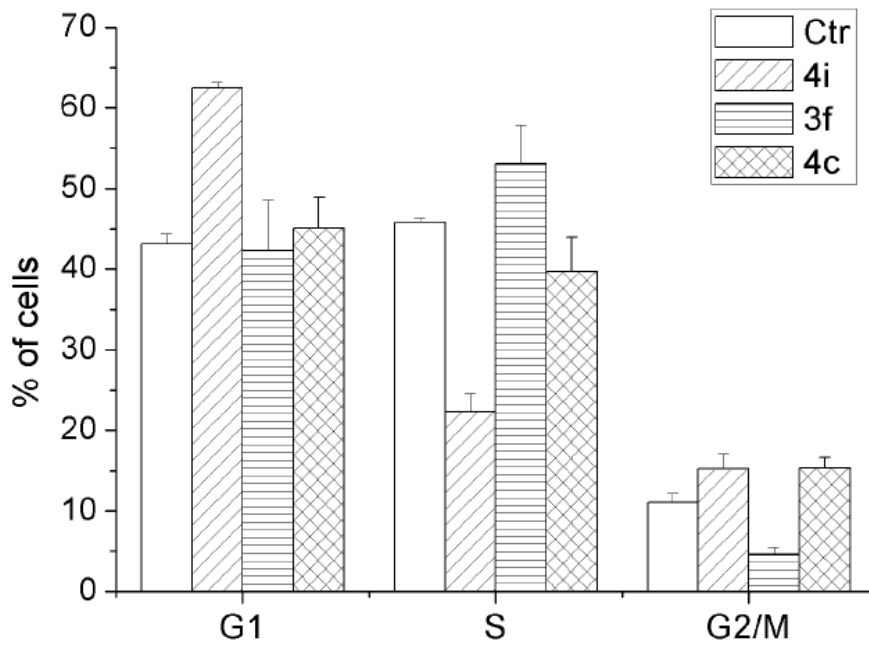


4d R = Me; R' = H (27%)

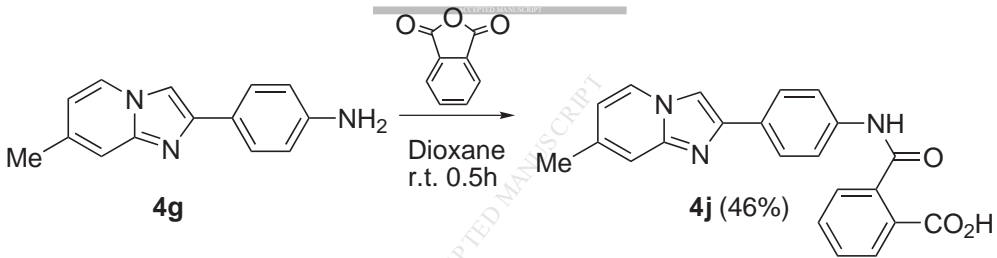
4i R = H; R' = Me (10%)

Scheme 4

Figure 5.

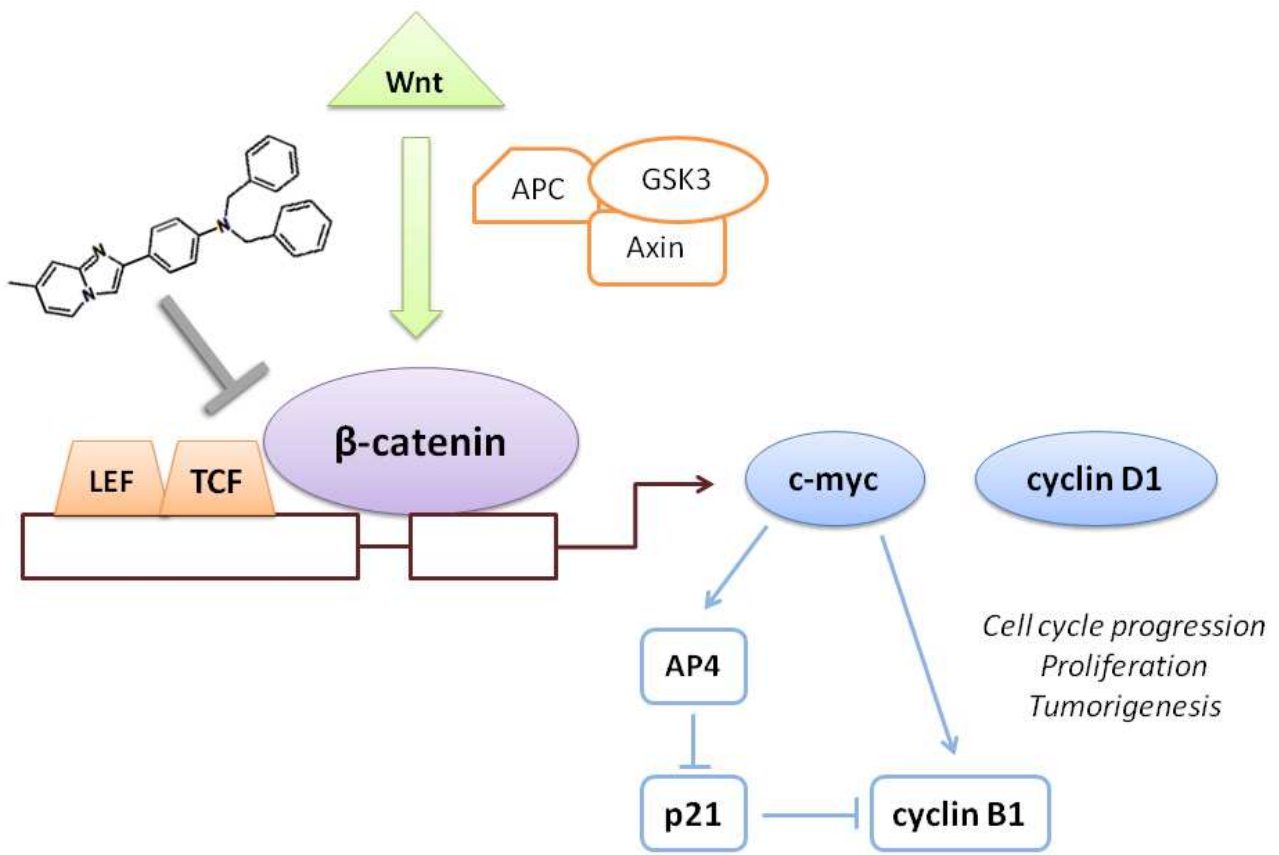


ACCEPTED MANUSCRIPT



Scheme 5

Figure 7



Highlights

- A series of imidazo[1,2-*a*]pyrimidines and imidazo[1,2-*a*]pyridines derivatives were synthesized
- Some compounds significantly inhibit the Wnt/ β -catenin pathway in a luciferase reporter assay
- Some compounds show similar cytotoxic potency in comparison to reference compounds
- One of the most active compounds **4i**, reduces the expression of Wnt-target genes in HT-29 cells
- *In vivo*, **4i** has an activity comparable to that of the reference compound IWR1.

□

Synthesis and biological evaluation of imidazo[1,2-*a*]pyrimidines and imidazo[1,2-*a*]pyridines as new inhibitors of the Wnt/ β -catenin signaling

Barbara Cosimelli, Sonia Laneri, Carmine Ostacolo, Antonia Sacchi, Elda Severi, Elena Porcù, Elena Rampazzo, Enrico Moro, Giuseppe Basso, Giampietro Viola

Contents:

Table 1SI. *In vitro* cell growth inhibition after 72 hours treatment of the newly investigated compounds.

Figure 1SI. Representative images of HT-29 cells treated with the compounds **3f**, **4a** and **4e**.

Spectroscopic data and elemental analysis results of all new synthesized compounds.

Representative ^1H and ^{13}C NMR spectra

Table 1SI. *In vitro* cell growth inhibition after 72 hours treatment of the newly investigated compounds.

Compound	GI ₅₀ (μM) ^a
	Human Primary Fibroblasts
3f	> 100
4c	> 100
4h	> 100
4i	52.3 ± 3.2

^a GI₅₀ indicates the required concentration to inhibit tumor cell proliferation by 50%. Data are expressed as the mean ± SEM from the dose–response curves of at least three independent experiments. n.d. not determined

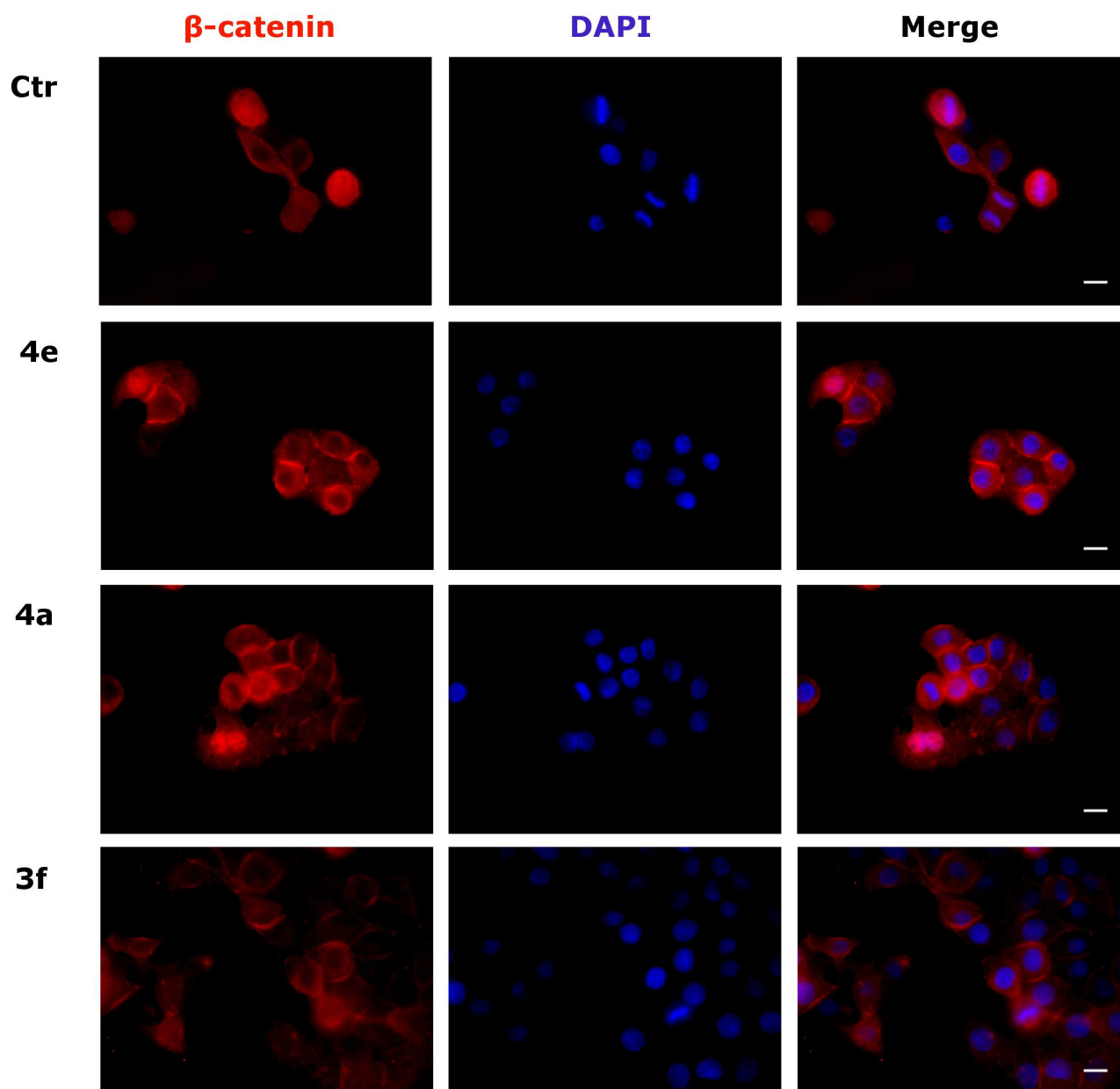


Figure 1Si. Representative images of HT-29 cells treated with the indicated compounds at 25 μ M for 24 hours. β -catenin (red) when it is detectable into the nucleus, otherwise it is localized in the cytoplasm. DAPI stained the nuclei (blue). Pictures were acquired by fluorescent microscope using a 60X objective (Bar=100 μ m).

Spectroscopic data and elemental analysis results of all new synthesized compounds:

2-(Benzylthio)-6-isobutoxypyrimidin-4-amine 1a: ^1H NMR ($[\text{D}_6]\text{DMSO}$, δ ppm): 7.42-7.35 (m, 2H, H-Ar); 7.31-7.18 (m, 3H, H-Ar); 6.70 (bs exch, 2H, NH_2); 5.42 (s, 1H, H-5); 4.29 (s, 2H, SCH_2); 3.93 (d, 2H, $J=6.2$ Hz, NCH_2); 1.99-1.88 (m, 1H, CH); 0.90 (d, 6H, $J=6.3$ Hz, $2\times\text{CH}_3$). ^{13}C NMR ($[\text{D}_6]\text{DMSO}$, δ ppm): 168.9; 168.6; 165.1; 138.6; 128.8; 128.3; 126.8; 81.7; 71.5; 33.8; 27.5; 18.9. ESI (m/z): 312.1 $[\text{M}+23]$. Anal. Calcd for $\text{C}_{15}\text{H}_{19}\text{N}_3\text{OS}$: C, 62.25; H, 6.62; N, 14.52 %. Found: C, 62.33; H, 6.71; N, 14.48 %.

N-[2-(Benzylthio)-6-isobutoxypyrimidin-4-yl]acetamide 1b: ^1H NMR ($[\text{D}_6]\text{DMSO}$, δ ppm): 10.76 (bs exch, 1H, NH); 7.44-7.42 (m, 2H, H-Ar); 7.33-7.31 (m, 2H, H-Ar); 7.26-7.24 (m, 1H, H-Ar); 7.12 (s, 1H, H-5); 4.39 (s, 2H, SCH_2); 4.06 (d, 2H, $J=6.6$ Hz, OCH_2); 2.09 (s, 3H, CH_3); 2.03-1.94 (m, 1H, CH); 0.93 (d, 6H, $J=6.6$ Hz, $2\times\text{CH}_3$). ^{13}C NMR ($[\text{D}_6]\text{DMSO}$, δ ppm): 170.5; 170.1; 169.1; 158.6; 138.0; 128.8; 128.4; 127.0; 89.5; 72.4; 34.0; 27.3; 24.1; 18.9. ESI (m/z): 354.0 $[\text{M}+23]$. Anal. Calcd for $\text{C}_{17}\text{H}_{21}\text{N}_3\text{O}_2\text{S}$: C, 61.61; H, 6.39; N, 12.68 %. Found: C, 61.85; H, 6.44; N, 12.55 %.

6-(Benzyloxy)-2-(benzylthio)pyrimidin-4-amine 1c: ^1H NMR ($[\text{D}_6]\text{DMSO}$, δ ppm): 7.40-7.14 (m, 10H, H-Ar); 6.78 (bs exch, 2H, NH_2); 5.50 (s, 1H, H-5); 5.29 (s, 2H, OCH_2); 4.30 (s, 2H, SCH_2). ^{13}C NMR ($[\text{D}_6]\text{DMSO}$, δ ppm): 168.7; 168.4; 165.2; 138.6; 137.0; 128.8; 128.4; 128.3; 127.8; 127.7; 126.8; 82.0; 66.8; 33.8. ESI (m/z): 346.2 $[\text{M}+23]$. Anal. Calcd for $\text{C}_{18}\text{H}_{17}\text{N}_3\text{OS}$: C, 66.85; H, 5.30; N, 12.99 %. Found: C, 66.95; H, 5.41; N, 12.70 %.

N-[6-(Benzyloxy)-2-(benzylthio)pyrimidin-4-yl]acetamide 1d: ^1H NMR ($[\text{D}_6]\text{DMSO}$, δ ppm): 10.78 (bs exch, 1H, NH); 7.42-7.21 (m, 10H, H-Ar); 7.18 (s, 1H, H-5); 5.38 (s, 2H, OCH_2); 4.39 (s, 2H, SCH_2); 2.08 (s, 3H, CH_3). ^{13}C NMR ($[\text{D}_6]\text{DMSO}$, δ ppm): 170.5; 169.6; 169.2; 158.7; 137.8; 136.3; 128.8; 128.4; 128.4; 128.0; 127.8; 127.0; 89.7; 67.8; 34.0; 24.0. ESI (m/z): 366.2 $[\text{M}+23]$. Anal. Calcd for $\text{C}_{20}\text{H}_{19}\text{N}_3\text{O}_2\text{S}$: C, 65.73; H, 5.24; N, 11.50 %. Found: C, 65.81; H, 5.29; N, 11.44 %.

6-Amino-2-(benzylthio)-3-isobutylpyrimidin-4(3H)-one 2a: ^1H NMR ($[\text{D}_6]\text{DMSO}$, δ ppm): 7.47-7.44 (m, 2H, H-Ar); 7.34-7.25 (m, 3H, H-Ar); 6.50 (bs exch, 2H, NH_2); 4.91 (s, 1H, H-5); 4.40 (s, 2H, SCH_2); 3.64 (d, 2H, $J=7.3$ Hz, NCH_2); 2.12-2.02 (m, 1H, CH); 0.81 (d, 6H, $J=6.6$ Hz, $2\times\text{CH}_3$). ^{13}C NMR ($[\text{D}_6]\text{DMSO}$, δ ppm): 161.7; 160.9; 160.4; 136.9; 129.3; 128.4; 127.3; 80.9; 48.9; 35.2; 27.2; 19.8. ESI (m/z): 312.0 $[\text{M}+23]$. Anal. Calcd for $\text{C}_{15}\text{H}_{19}\text{N}_3\text{OS}$: C, 62.25; H, 6.62; N, 14.52 %. Found: C, 62.36; H, 6.70; N, 14.45 %.

N-[2-(Benzylthio)-1-isobutyl-6-oxo-1,6-dihydropyrimidin-4-yl]acetamide 2b: ^1H NMR ($[\text{D}_6]\text{DMSO}$, δ ppm): 10.30 (bs exch, 1H, NH); 7.48 (pd, 2H, H-Ar); 7.36-7.27 (m, 3H, H-Ar); 6.75

(s, 1H, H-5); 4.53 (s, 2H, SCH₂); 3.73 (d, 2H, *J*=7.5 Hz, NCH₂); 2.12 (s, 3H, CH₃); 2.15-2.05 (m, 1H, CH); 0.82 (d, 6H, *J*=6.6 Hz, 2xCH₃). ¹³C NMR ([D₆]DMSO, δ ppm): 170.2; 162.3; 161.1; 153.4; 136.5; 129.2; 128.6; 127.5; 92.3; 49.9; 35.5; 26.9; 24.2; 19.7. ESI (m/z): 331.8 [M+1]. Anal. Calcd for C₁₇H₂₁N₃O₂S: C, 61.61; H, 6.39; N, 12.68 %. Found: C, 61.90; H, 6.48; N, 12.54 %.

6-Amino-3-benzyl-2-(benzylthio)pyrimidin-4(3H)-one 2c: ¹H NMR ([D₆]DMSO, δ ppm): 7.42-7.39 (m, 2H, H-Ar); 7.31-7.23 (m, 6H, H-Ar); 7.21-7.13 (m, 2H, H-Ar); 6.62 (bs exch, 2H, NH₂); 5.08 (s, 2H, NCH₂); 5.01 (s, 1H, H-5); 4.37 (s, 2H, SCH₂). ¹³C NMR ([D₆]DMSO, δ ppm): 161.6; 161.3; 160.8; 136.8; 136.4; 129.3; 128.4; 128.4; 127.3; 127.1; 126.6; 80.6; 45.1; 35.1. ESI (m/z): 345.9 [M+23]. Anal. Calcd for C₁₈H₁₇N₃OS: C, 66.85; H, 5.30; N, 12.99 %. Found: C, 66.99; H, 5.44; N, 12.66 %.

N-[1-Benzyl-2-(benzylthio)-6-oxo-1,6-dihydropyrimidin-4-yl]acetamide 2d: ¹H NMR ([D₆]DMSO, δ ppm): 10.40 (bs exch, 1H, NH); 7.44-7.40 (m, 2H, H-Ar); 7.31-7.24 (m, 6H, H-Ar); 7.17-7.14 (m, 2H, H-Ar); 6.84 (s, 1H, H-5); 5.14 (s, 2H, NCH₂); 4.49 (s, 2H, SCH₂); 2.14 (s, 3H, CH₃). ¹³C NMR ([D₆]DMSO, δ ppm): 170.4; 162.4; 161.5; 153.8; 136.4; 135.4; 129.2; 128.6; 128.5; 127.6; 127.4; 126.7; 92.3; 46.2; 35.5; 24.2. ESI (m/z): 366.2 [M+23]. Anal. Calcd for C₂₀H₁₉N₃O₂S: C, 65.73; H, 5.24; N, 11.50 %. Found: C, 65.87; H, 5.20; N, 11.55 %.

5,7-Dimethoxy-2-(4-nitrophenyl)imidazo[1,2-a]pyrimidine 3a: ¹H NMR ([D₆] DMSO, δ ppm): 8.37 (s, 1H, H-3); 8.28-8.26 (m, 2H, H-Ar); 8.23-8.21 (m, 2H, H-Ar); 6.19 (s, 1H, H-6); 4.16 (s, 3H, 7-OCH₃); 3.96 (s, 3H, 5-OCH₃). ¹³C NMR ([D₆]DMSO, δ ppm): 165.51; 156.3; 150.3; 146.3; 140.5; 140.4; 126.0; 124.0; 105.2; 78.3; 57.8; 54.0. Anal. Calcd for C₁₄H₁₂N₄O₄: C, 56.00; H, 4.03; N, 18.66 %. Found: C, 56.20; H, 4.15; N, 18.44 %.

4-(5,7-Dimethoxyimidazo[1,2-a]pyrimidin-2-yl)aniline 3b: ¹H NMR ([D₆] DMSO, δ ppm): 7.69 (s, 1H, H-3); 7.50 (pd, 2H, H-Ar); 6.58 (pd, 2H, H-Ar); 5.46 (s, 2H, NH₂); 5.13 (s, 1H, H-6); 3.81 (s, 3H, 7-OCH₃); 3.31 (s, 3H, 5-OCH₃). ¹³C NMR ([D₆]DMSO, δ ppm): 169.8; 158.1; 150.3; 147.0; 131.0; 126.9; 115.2; 114.4; 100.7; 79.9; 54.5; 54.0. Anal. Calcd for C₁₄H₁₄N₄O₂: C, 62.21; H, 5.22; N, 20.73 %. Found: C, 62.10; H, 5.12; N, 20.69 %.

4-(5,7-Dimethoxyimidazo[1,2-a]pyrimidin-2-yl)-N-methylaniline 3c: ¹H NMR ([D₆] DMSO, δ ppm): 7.71 (s, 1H, H-3); 7.60 (pd, 2H, H-Ar); 6.57 (pd, 2H, H-Ar); 6.07 (s, 1H, H-6); 5.21 (bs exch, 1H, NH); 4.12 (s, 3H, 7-OCH₃); 3.92 (s, 3H, 5-OCH₃); 2.49 (s, 3H, CH₃). ¹³C NMR ([D₆]DMSO, δ ppm): 164.5; 155.9; 148.6; 147.9; 144.1; 126.3; 121.3; 113.7; 98.9; 76.9; 57.5; 53.7; 18.1. Anal. Calcd for C₁₅H₁₆N₄O₂: C, 63.37; H, 5.67; N, 19.71 %. Found: C, 63.15; H, 5.61; N, 19.64 %.

N-Benzyl-4-(5,7-dimethoxyimidazo[1,2-a]pyrimidin-2-yl)aniline 3d: ^1H NMR ($[\text{D}_6]$ DMSO, δ ppm): 7.69 (s, 1H, H-3); 7.62 (pd, 2H, H-Ar); 7.36-7.34 (m, 2H, H-Ph); 7.32-7.30 (m, 2H, H-Ph); 7.29-7.27 (m, 1H, H-Ph), 6.57 (pd, 2H, H-Ar); 6.40 (t, $J=5.7$ Hz, 1H, NH); 6.04 (s, 1H, H-6); 4.28 (d, $J=5.7$ Hz, 2H, CH_2); 4.09 (s, 3H, 7- OCH_3); 3.90 (s, 3H, 5- OCH_3). ^{13}C NMR ($[\text{D}_6]$ DMSO, δ ppm): 164.5; 155.9; 148.4; 148.3; 144.0; 140.2; 128.2; 127.1; 126.7; 126.3; 121.5; 112.2; 99.1; 77.0; 57.5; 53.7; 46.3. Anal. Calcd for $\text{C}_{21}\text{H}_{20}\text{N}_4\text{O}_2$: C, 69.98; H, 5.59; N, 15.55 %. Found: C, 69.87; H, 5.45; N, 15.51 %.

N,N-Dibenzyl-4-(5,7-dimethoxyimidazo[1,2-a]pyrimidin-2-yl)aniline 3e: ^1H NMR ($[\text{D}_6]$ DMSO, δ ppm): 7.73 (s, 1H, H-3); 7.67 (pd, 2H, H-Ar); 7.32-7.26 (m, 10H, H-Ph), 6.70 (pd, 2H, H-Ar); 6.05 (s, 1H, H-6); 4.73 (s, 4H, $2\times\text{CH}_2$); 4.10 (s, 3H, 7- OCH_3); 3.91 (s, 3H, 5- OCH_3). ^{13}C NMR ($[\text{D}_6]$ DMSO, δ ppm): 164.6; 155.9; 147.8; 143.6; 138.9; 129.6; 128.5; 126.7; 126.6; 126.4; 121.8; 112.3; 99.4; 77.1; 57.5; 54.1; 53.7. Anal. Calcd for $\text{C}_{28}\text{H}_{26}\text{N}_4\text{O}_2$: C, 74.65; H, 5.82; N, 12.44 %. Found: C, 74.36; H, 5.76; N, 12.41 %.

5-(Benzyloxy)-7-methyl-2-(4-nitrophenyl)imidazo[1,2-a]pyrimidine 3g: ^1H NMR ($[\text{D}_6]$ DMSO, δ ppm): 8.49 (s, 1H, H-3); 8.26-8.24 (m, 2H, H-Ar); 8.20-8.18 (m, 2H, H-Ar); 7.38-7.36 (m, 2H, H-Ph); 7.34-7.27 (m, 3H, H-Ph); 5.88 (s, 1H, H-6); 5.64 (s, 2H, CH_2); 2.36 (s, 3H, CH_3). ^{13}C NMR ($[\text{D}_6]$ DMSO, δ ppm): 156.1; 152.6; 146.4; 144.9; 139.5; 138.1; 135.9, 128.9; 127.6; 126.3; 126.1; 124.0; 108.4; 97.3; 49.1; 18.7. Anal. Calcd for $\text{C}_{20}\text{H}_{16}\text{N}_4\text{O}_3$: C, 66.66; H, 4.48; N, 15.55 %. Found: C, 66.56; H, 4.35; N, 15.49 %.

N-Benzyl-4-(6-methylimidazo[1,2-a]pyridin-2-yl)aniline 4c: ^1H NMR ($[\text{D}_6]$ DMSO, δ ppm): 8.25 (s, 1H, H-3), 8.02 (s, 1H, H-5), 7.63 (pd, 2H, H-Ar), 7.39-7.32 (m, 6H, H-Ph and H-8); 7.23 (d, $J=7.5$ Hz, 1H, H-7); 7.03 (d, $J=8.8$ Hz, H-7), 6.62 (pd, 2H, H-Ar), 6.43 (m, 1H, NH); 4.30 (d, $J=5.5$ Hz, 2H, CH_2); 2.26 (s, 3H, CH_3). ^{13}C NMR ($[\text{D}_6]$ DMSO, δ ppm): 148.4; 145.3; 143.6; 140.2; 128.3; 127.2; 127.0; 126.6; 126.4; 123.9; 121.8; 120.8; 115.5; 112.2; 106.5; 46.4, 17.5. Anal. Calcd for $\text{C}_{21}\text{H}_{19}\text{N}_3$: C, 80.48; H, 6.11; N, 13.41 %. Found: C, 80.30; H, 6.45; N, 13.51 %.

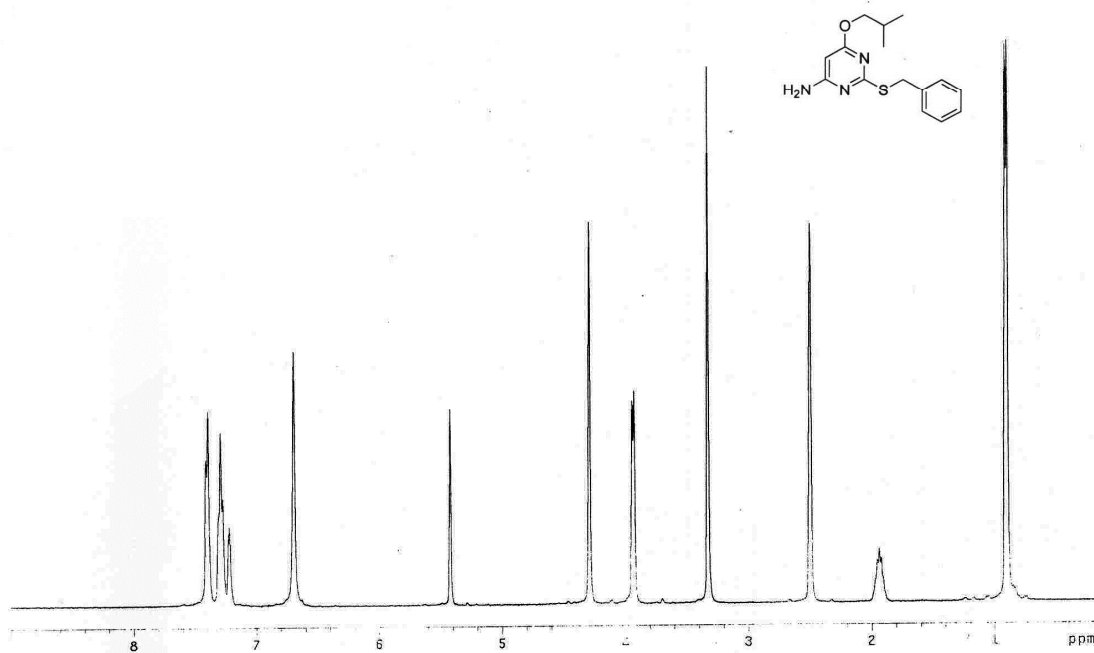
N,N-Dibenzyl-4-(6-methylimidazo[1,2-a]pyridin-2-yl)aniline 4d: ^1H NMR ($[\text{D}_6]$ DMSO, δ ppm): ^1H NMR ($[\text{D}_6]$ DMSO, δ ppm): 8.24 (s, 1H, H-3), 8.03 (s, 1H, H-5), 7.67 (pd, 2H, H-Ar), 7.40 (d, $J=9.2$ Hz, 1H, H-8), 7.36-7.22 (m, 10H, H-Ph); 7.02 (d, $J=9.2$ Hz, H-7); 6.73 (pd, 2H, H-Ar), 4.74 (s, 4H, $2\times\text{CH}_2$); 2.25 (s, 3H, CH_3). ^{13}C NMR ($[\text{D}_6]$ DMSO, δ ppm): 147.8; 145.0; 143.7; 138.9; 128.5; 127.1; 126.8; 126.6; 126.5; 123.9; 122.2; 120.9; 115.6; 112.4; 106.8; 54.1, 17.5. Anal. Calcd for $\text{C}_{28}\text{H}_{25}\text{N}_3$: C, 83.34; H, 6.24; N, 10.41 %. Found: C, 83.56; H, 6.48; N, 9.98 %.

N-Benzyl-4-(7-methylimidazo[1,2-a]pyridin-2-yl)aniline 4h: ^1H NMR ($[\text{D}_6]$ DMSO, δ ppm): 8.30 (d, $J=6.8$ Hz, 1H, H-5); 7.98 (s, 1H, H-3); 7.59 (pd, 2H, H-Ar), 7.35-7.19 (m, 6H, H-Ph and H-8); 6.64 (d, $J=6.8$ Hz, 1H, H-6); 6.60 (pd, 2H, H-Ar), 6.38 (t, $J=6.0$ Hz, 1H, NH); 4.28 (d, $J=6.0$

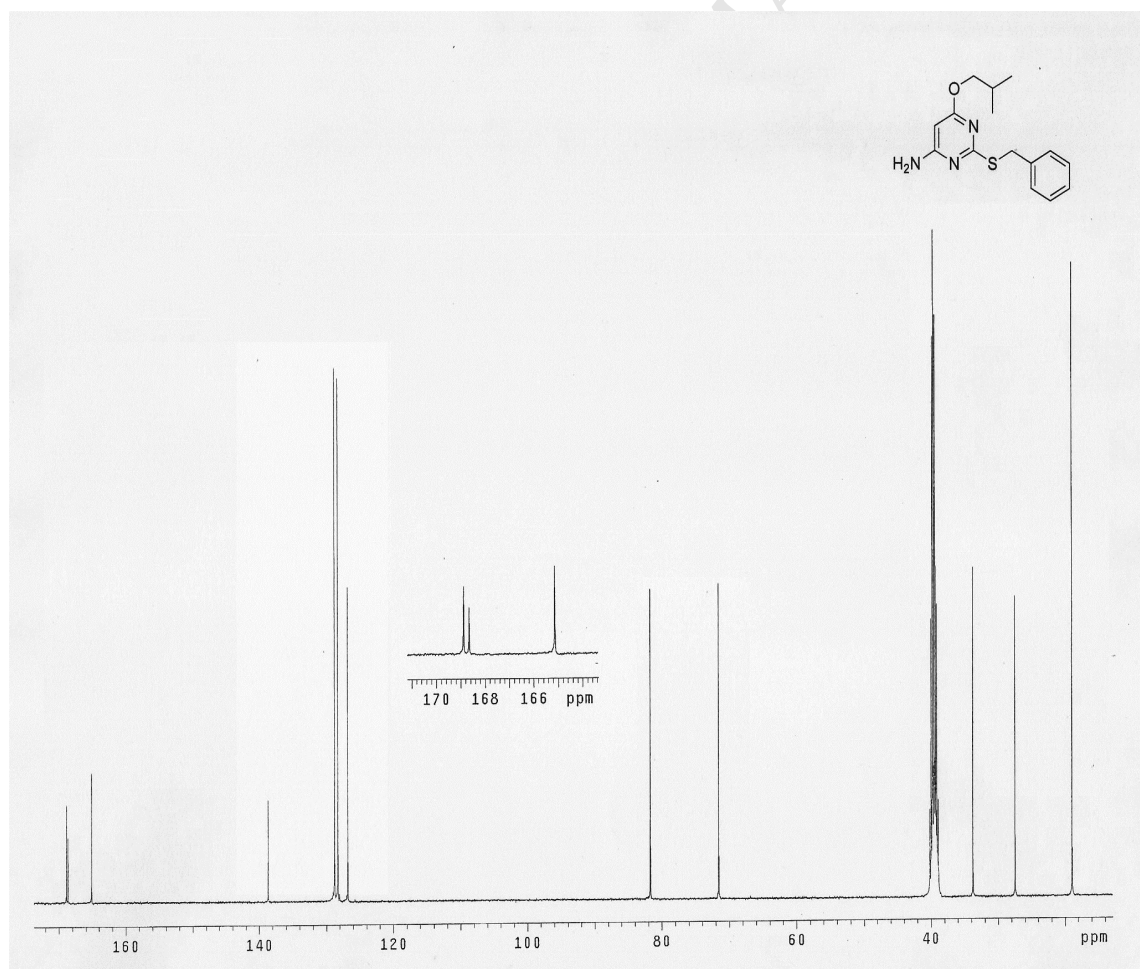
Hz, 2H, CH₂); 2.30 (s, 3H, CH₃). ¹³C NMR ([D₆]DMSO, δ ppm): 148.4; 145.3; 145.0; 140.2; 134.4; 128.3; 127.2; 126.6; 126.4; 125.7; 121.9; 114.5; 114.1; 112.3; 106.1; 46.4, 20.8. Anal. Calcd for C₂₁H₁₉N₃: C, 80.48; H, 6.11; N, 13.41 %. Found: C, 80.20; H, 6.28; N, 13.66 %.

***N,N*-Dibenzyl-4-(7-methylimidazo[1,2-*a*]pyridin-2-yl)aniline 4i:** ¹H NMR ([D₆] DMSO, δ ppm): 8.28 (d, *J*=6.8 Hz, 1H, H-5); 8.01 (s, 1H, H-3); 7.65 (pd, 2H, H-Ar), 7.32-7.22 (m, 11H, H-Ph and H-8); 6.72 (pd, 2H, H-Ar), 6.70 (d, *J*=6.8 Hz, 1H, H-6); 4.72 (s, 4H, 2xCH₂); 2.31 (s, 3H, CH₃). ¹³C NMR ([D₆]DMSO, δ ppm): 147.9; 144.9; 144.7; 138.9; 134.9; 128.8; 128.5; 126.8; 126.6; 126.5; 125.7; 122.0; 114.4; 112.4; 106.5; 54.1, 20.8. Anal. Calcd for C₂₈H₂₅N₃: C, 83.34; H, 6.24; N, 10.41 %. Found: C, 83.20; H, 6.18; N, 10.36 %.

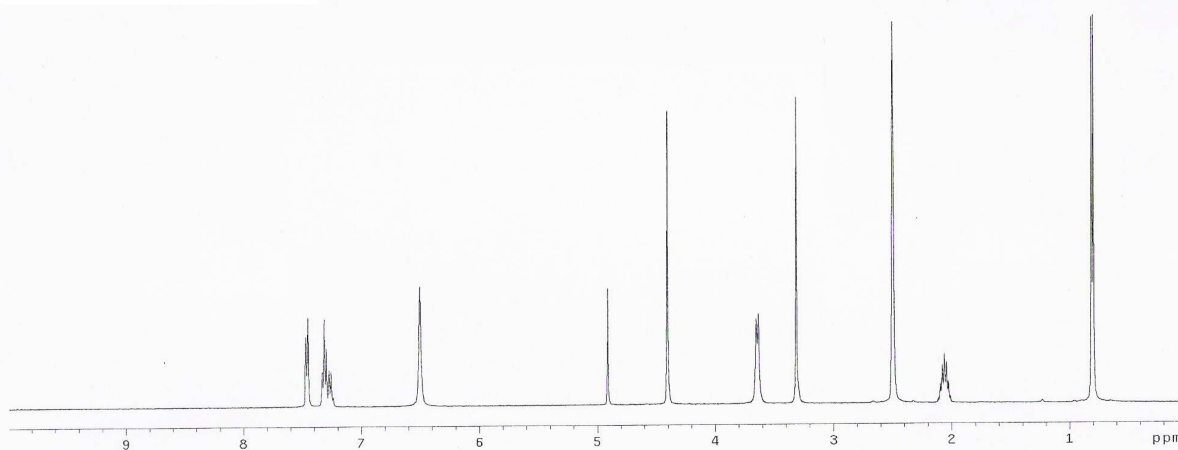
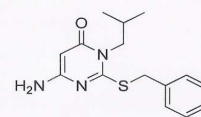
2-[[4-(7-Methylimidazo[1,2-*a*]pyridin-2-yl)phenyl]carbonyl] benzoic acid 4j: ¹H NMR ([D₆] DMSO, δ ppm): 10.66 (bs exch, 1H, NH); 8.76 (d, *J*=6.8 Hz, 1H, H-5); 8.65 (s, 1H, H-3); 7.98 (pd, 2H, H-Ar), 7.94-7.87 (m, 3H, H-Ar and H-Ph); 7.74 (m, 1H, H-8); 7.68-7.56 (m, 3H, H-Ph); 7.35 (d, *J*=6.8 Hz, 1H, H-6); 2.54 (s, 3H, CH₃). ¹³C NMR ([D₆]DMSO, δ ppm): 167.8; 167.3; 145.3; 141.3; 140.2; 138.6; 134.8; 131.9; 130.8; 129.9; 129.6; 129.6; 128.2; 127.8; 126.8; 121.1; 119.8; 119.5; 109.9; 21.2. Anal. Calcd for C₂₂H₁₇N₃O₃: C, 71.15; H, 4.61; N, 11.33 %. Found: C, 71.52; H, 4.43; N, 11.25 %.



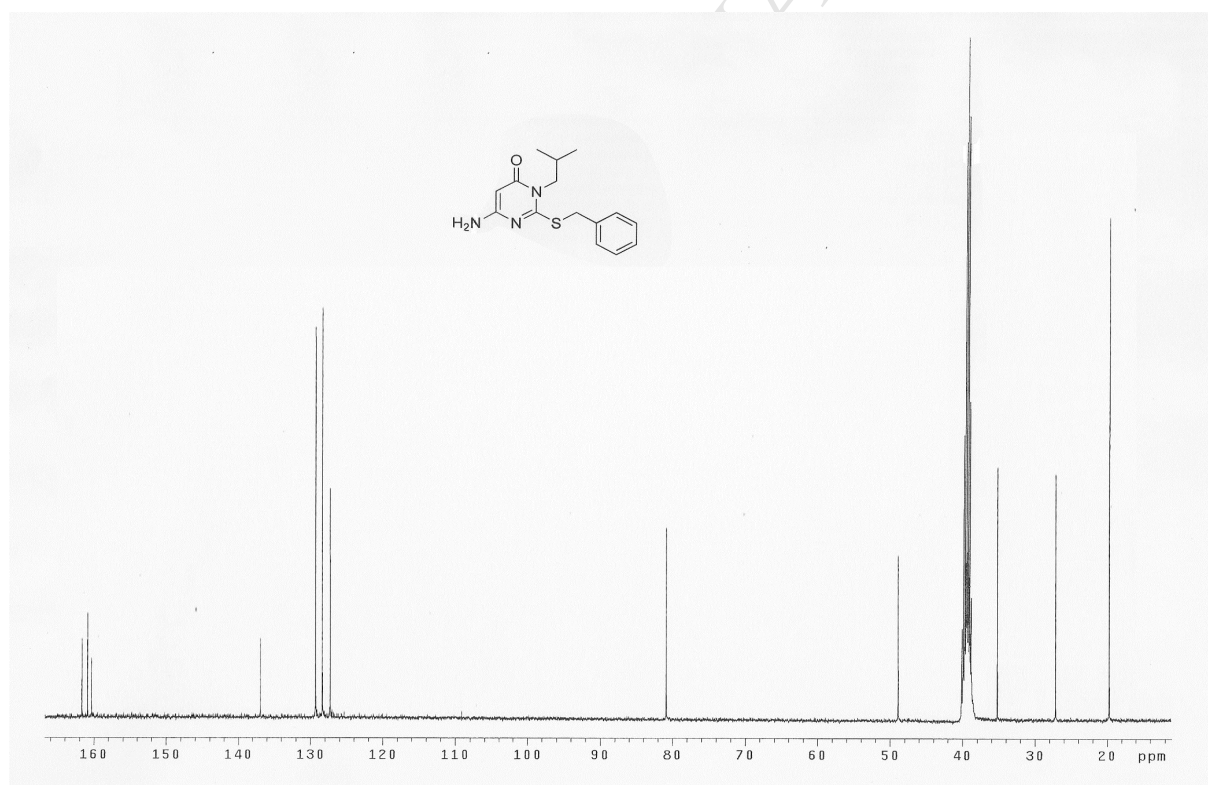
^1H NMR ($\text{DMSO-}d_6$) of **1a**.



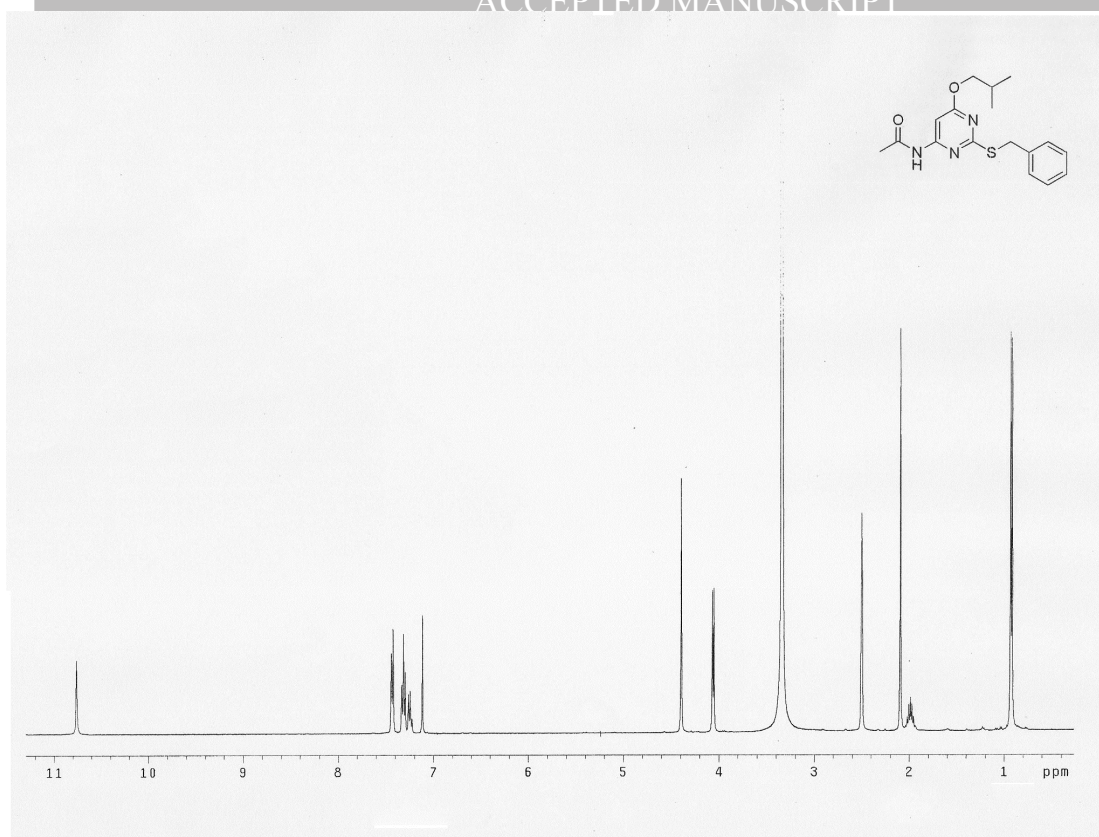
^{13}C NMR ($\text{DMSO-}d_6$) of **1a**.



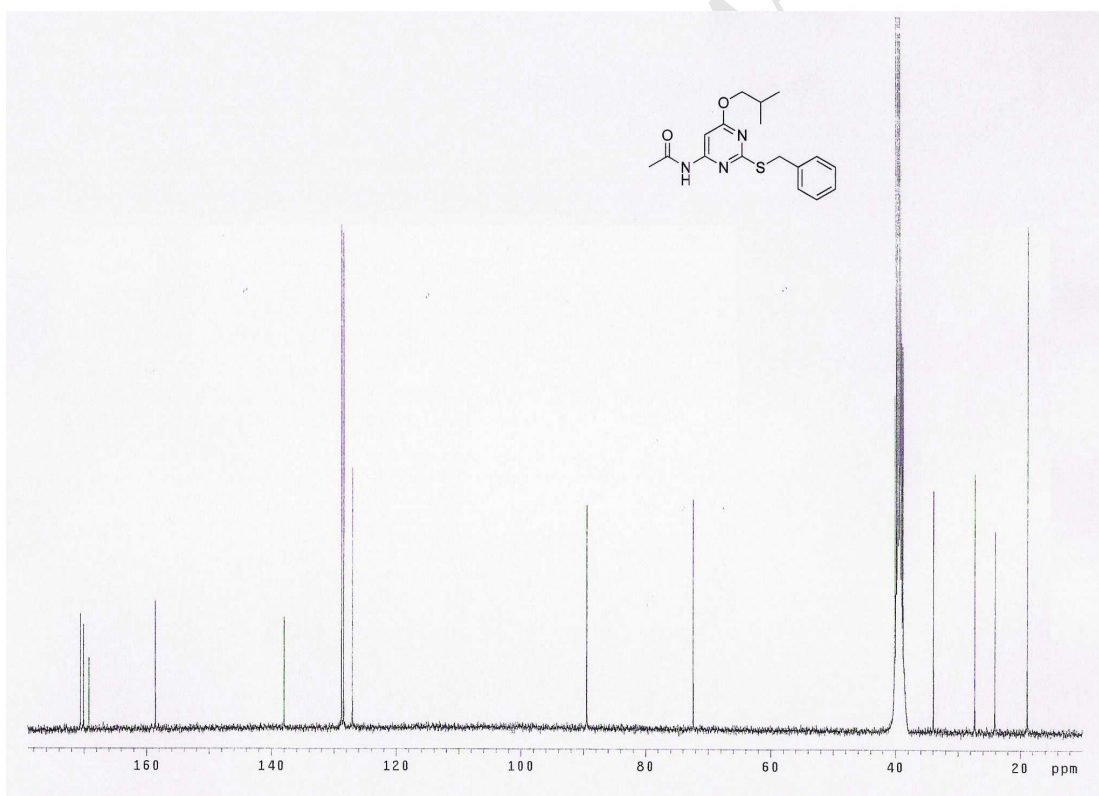
^1H NMR (DMSO- d_6) of **2a**.



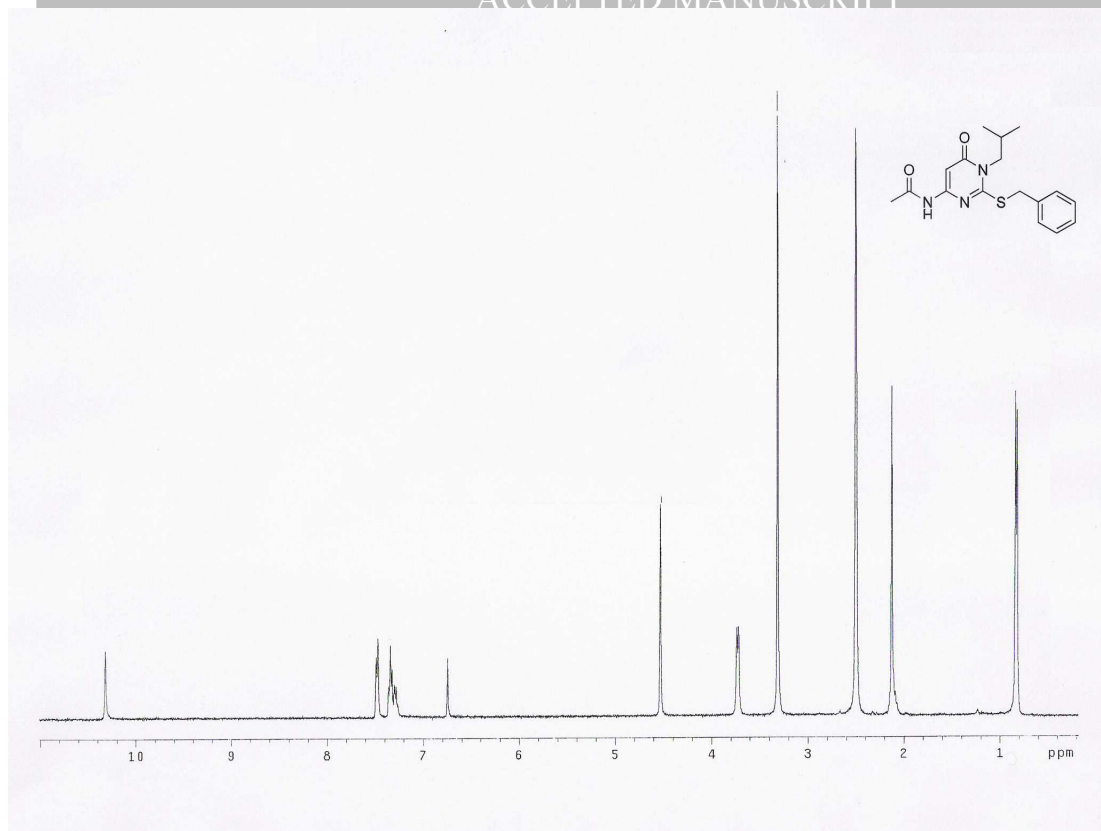
^{13}C NMR (DMSO- d_6) of **2a**.



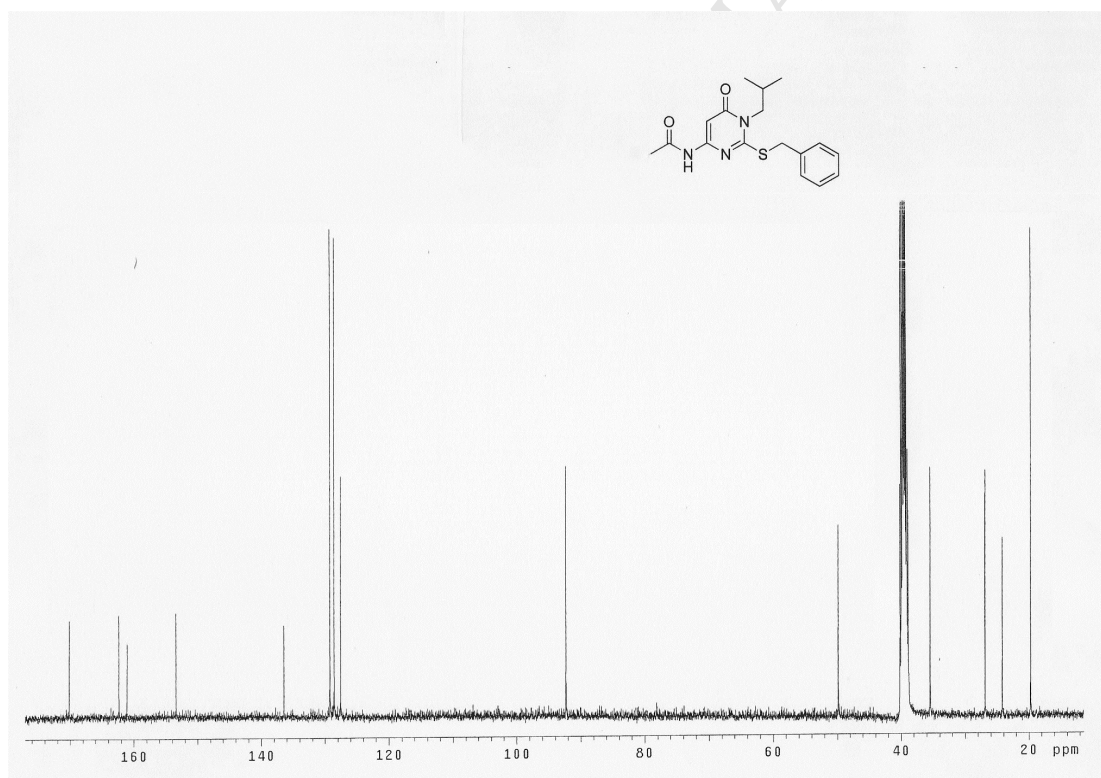
^1H NMR (DMSO- d_6) of **1b**.



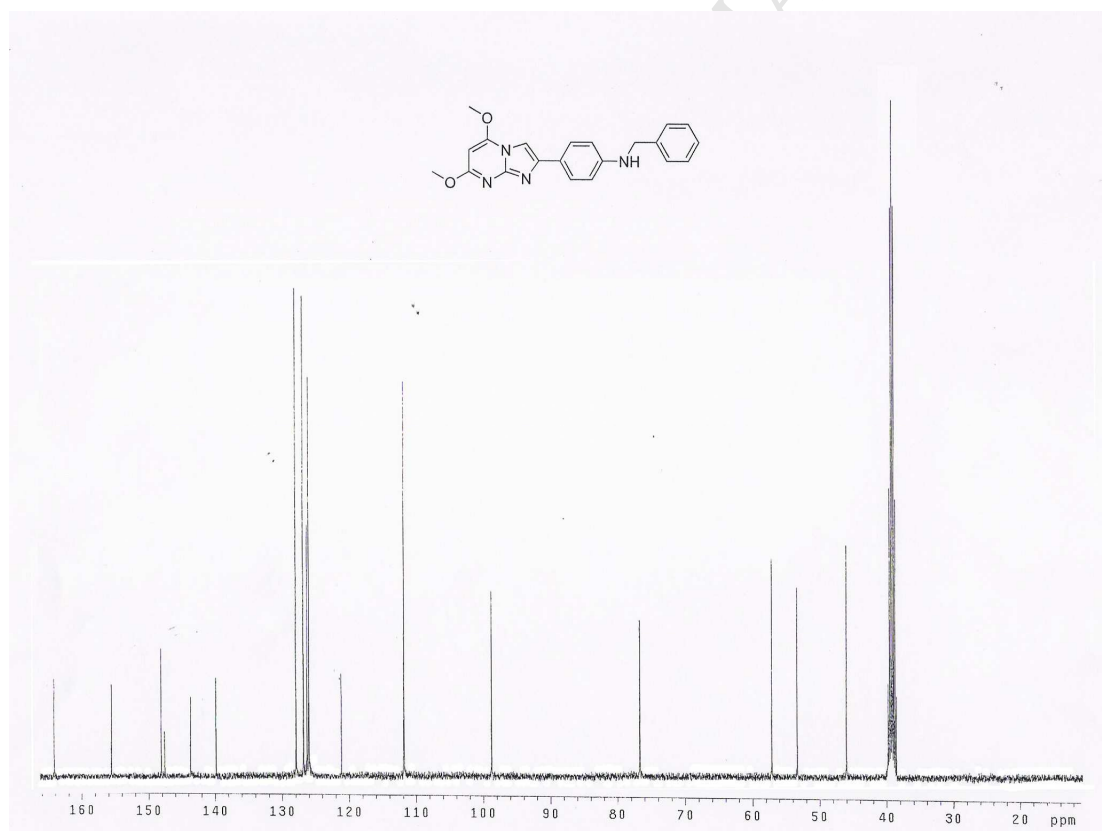
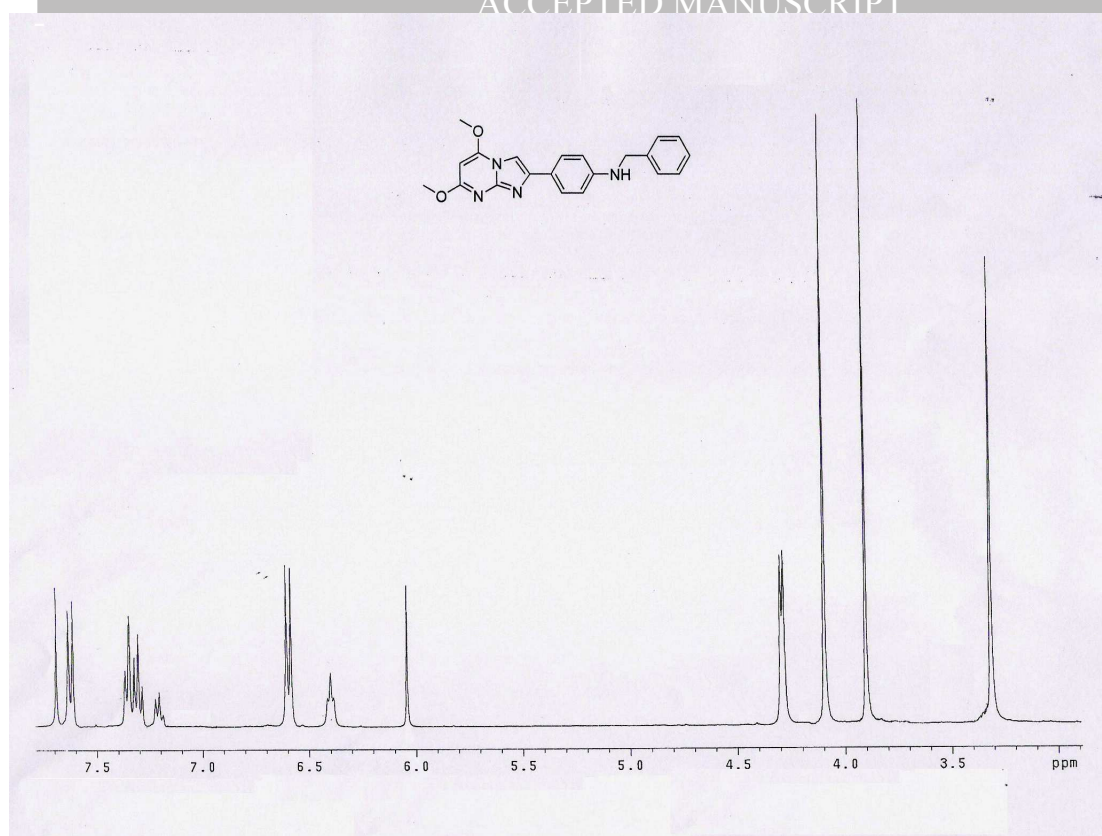
^{13}C NMR (DMSO- d_6) of **1b**.

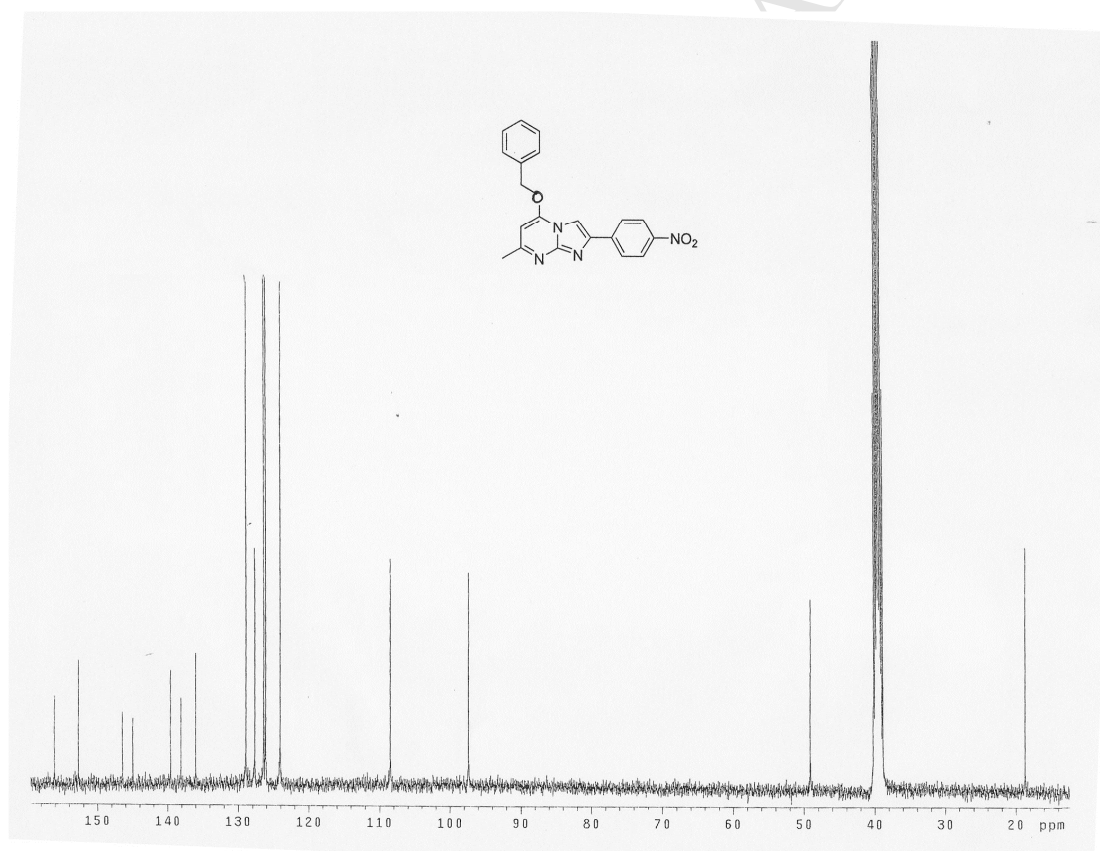
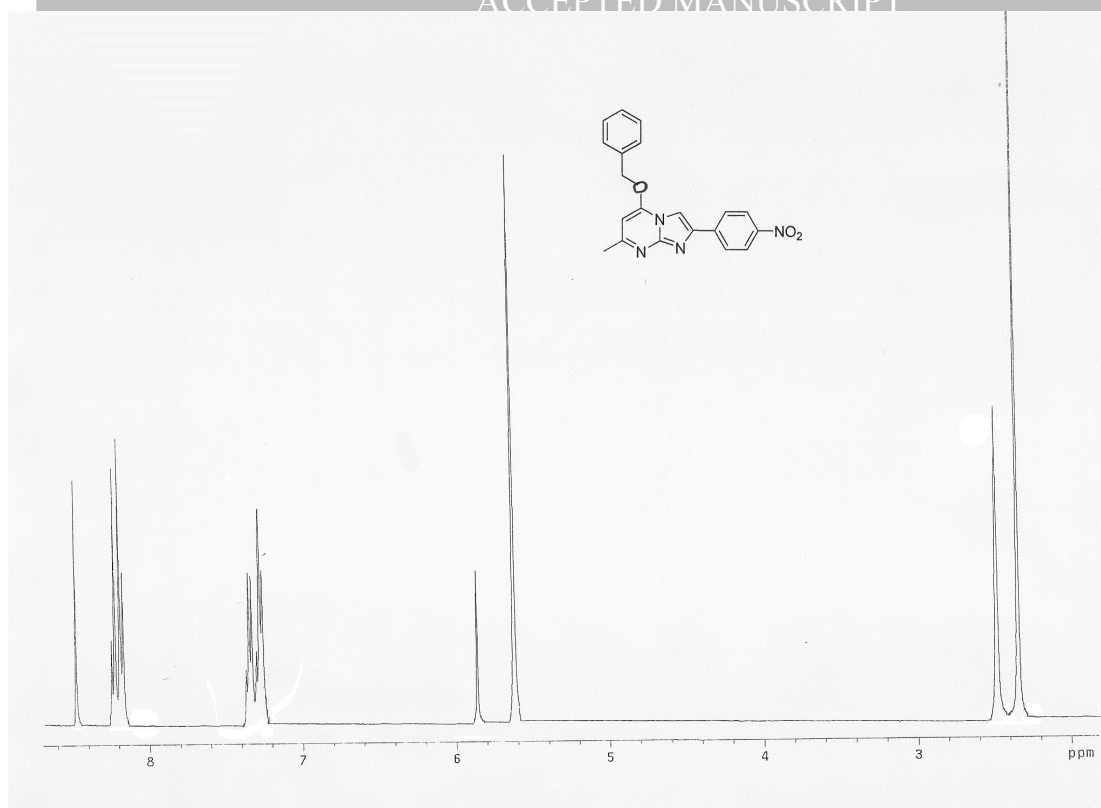


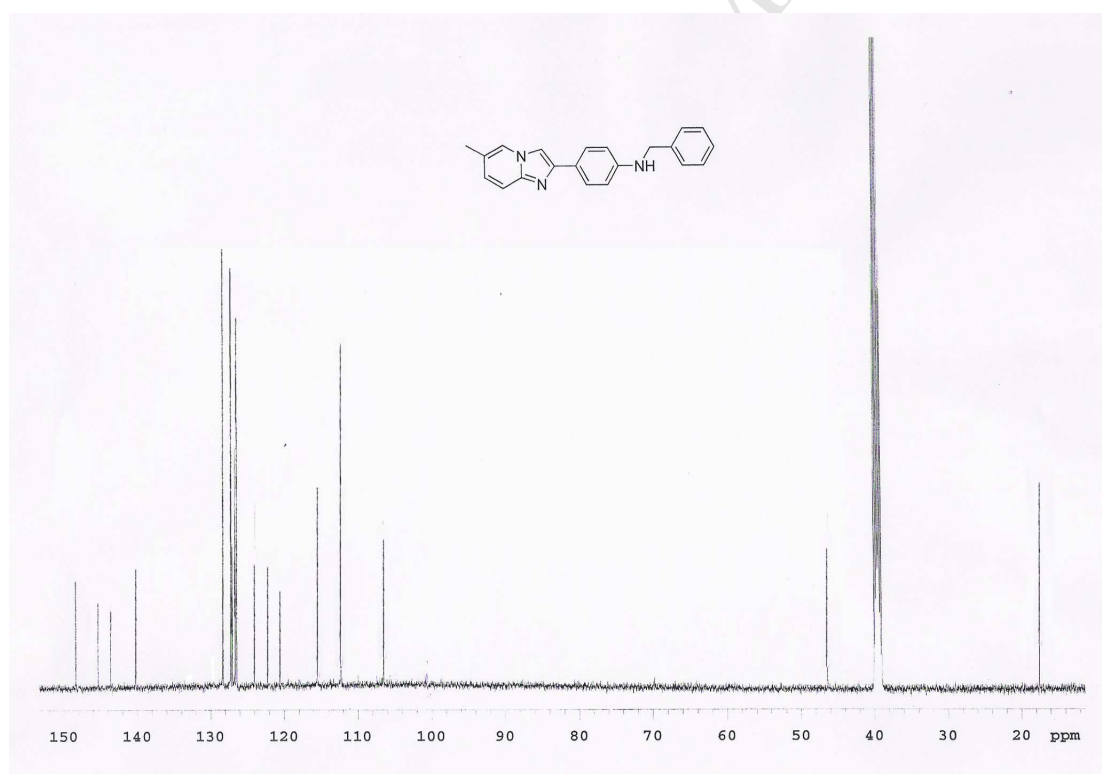
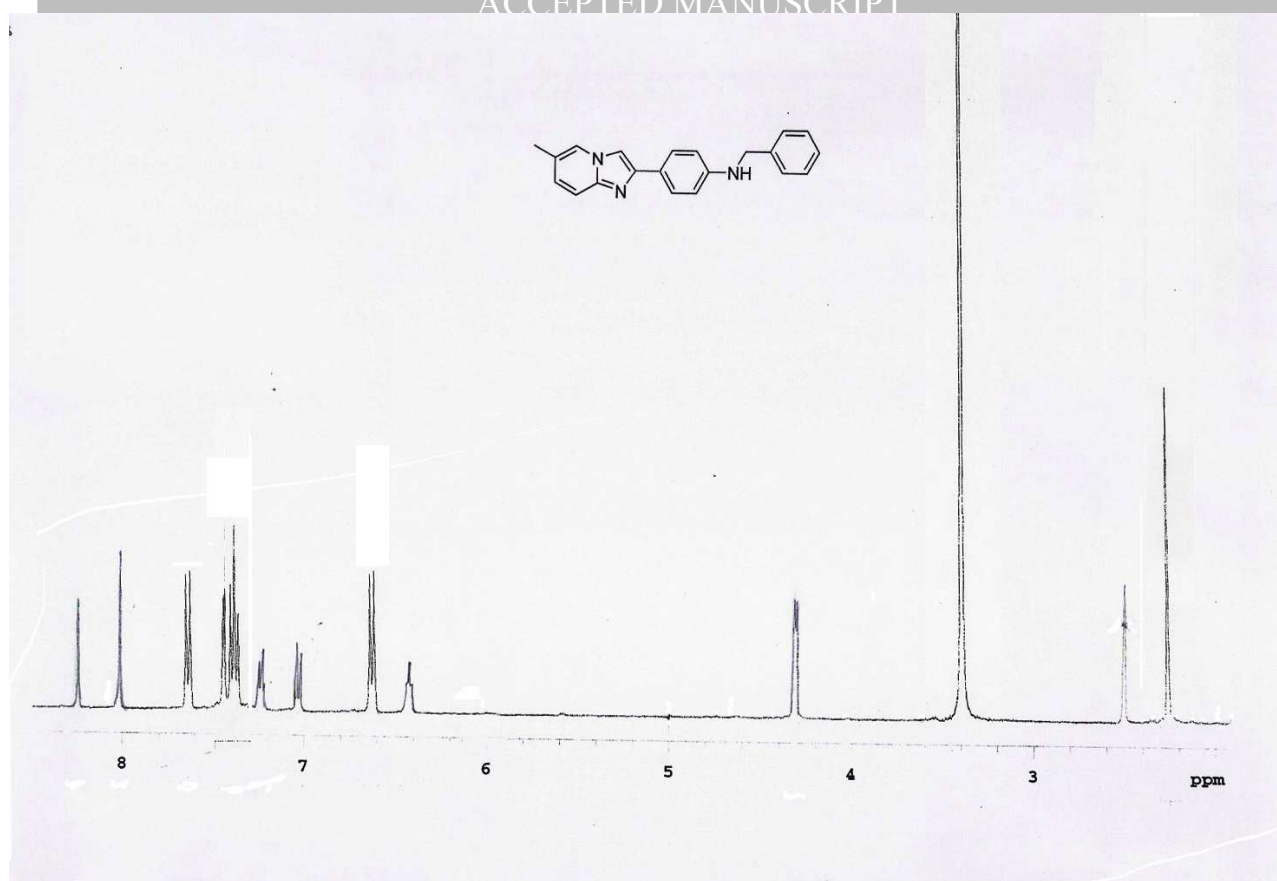
^1H NMR (DMSO- d_6) of **2b**.

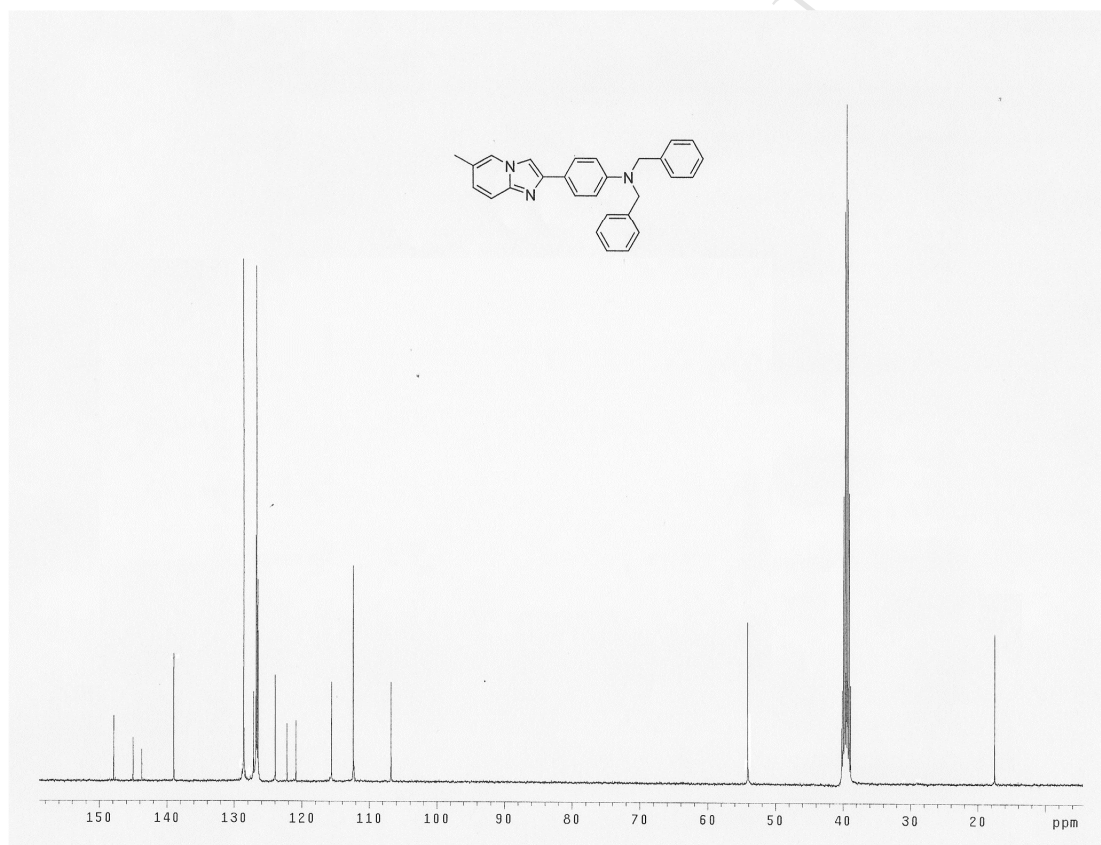
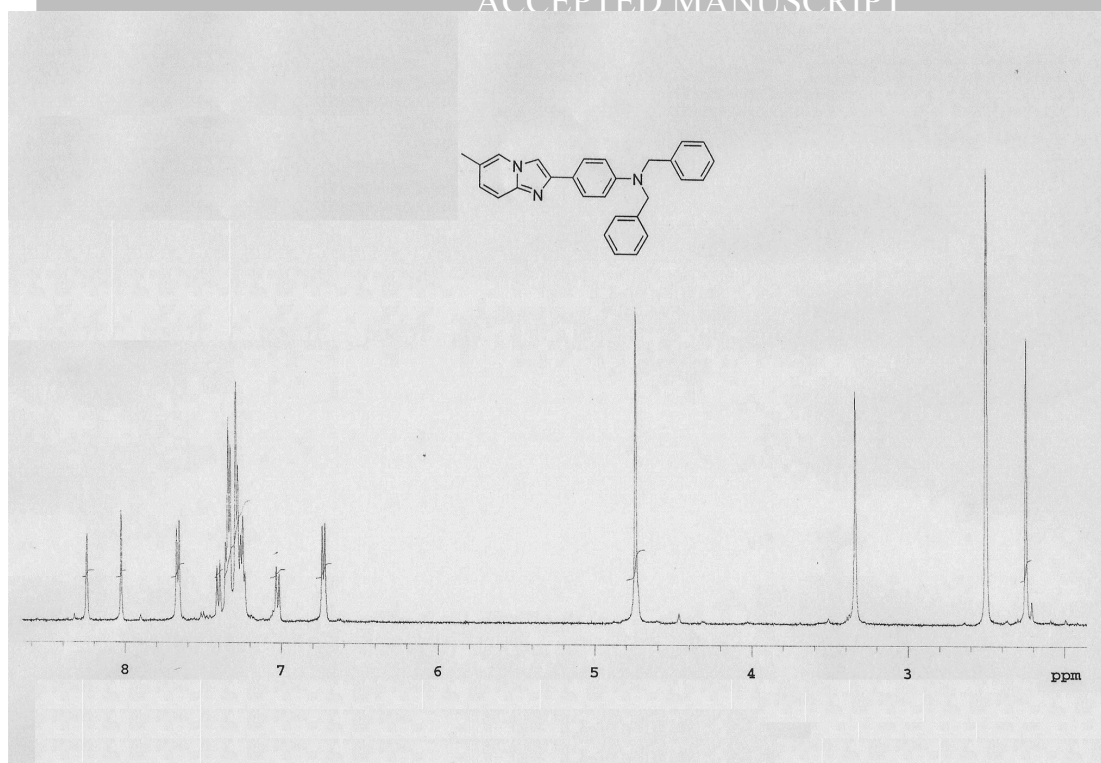


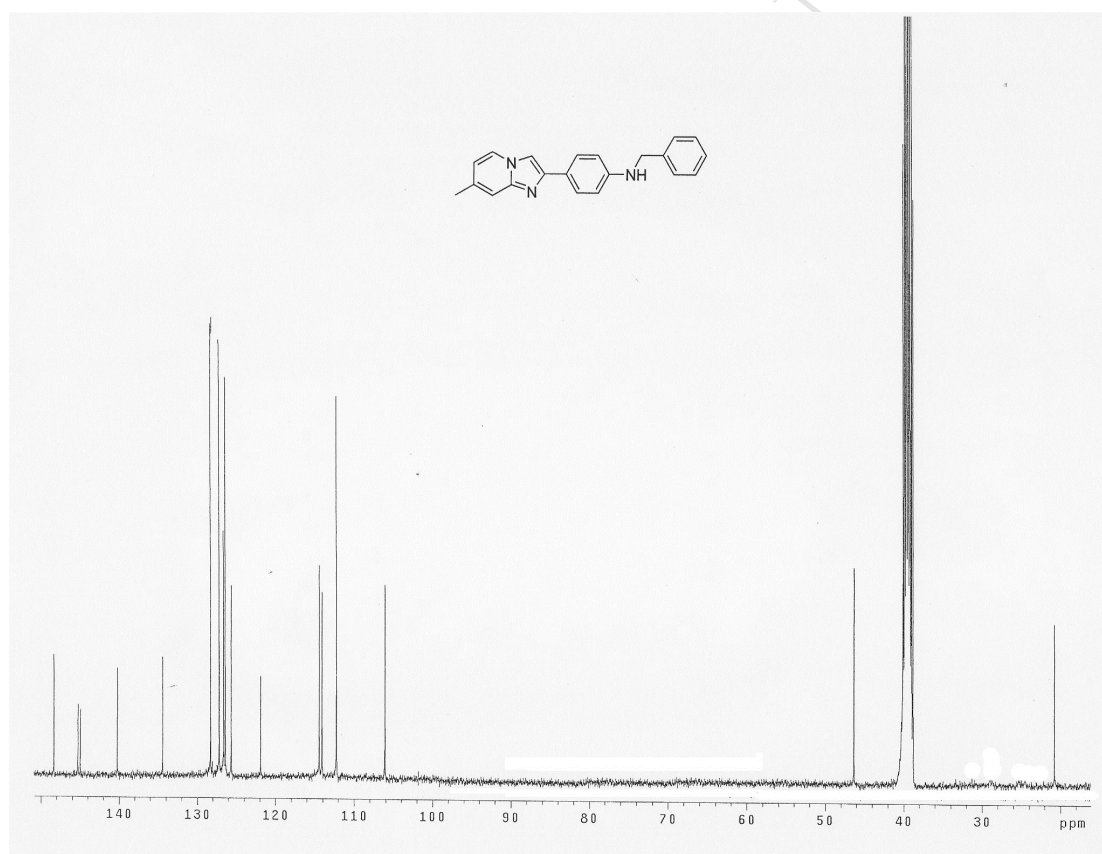
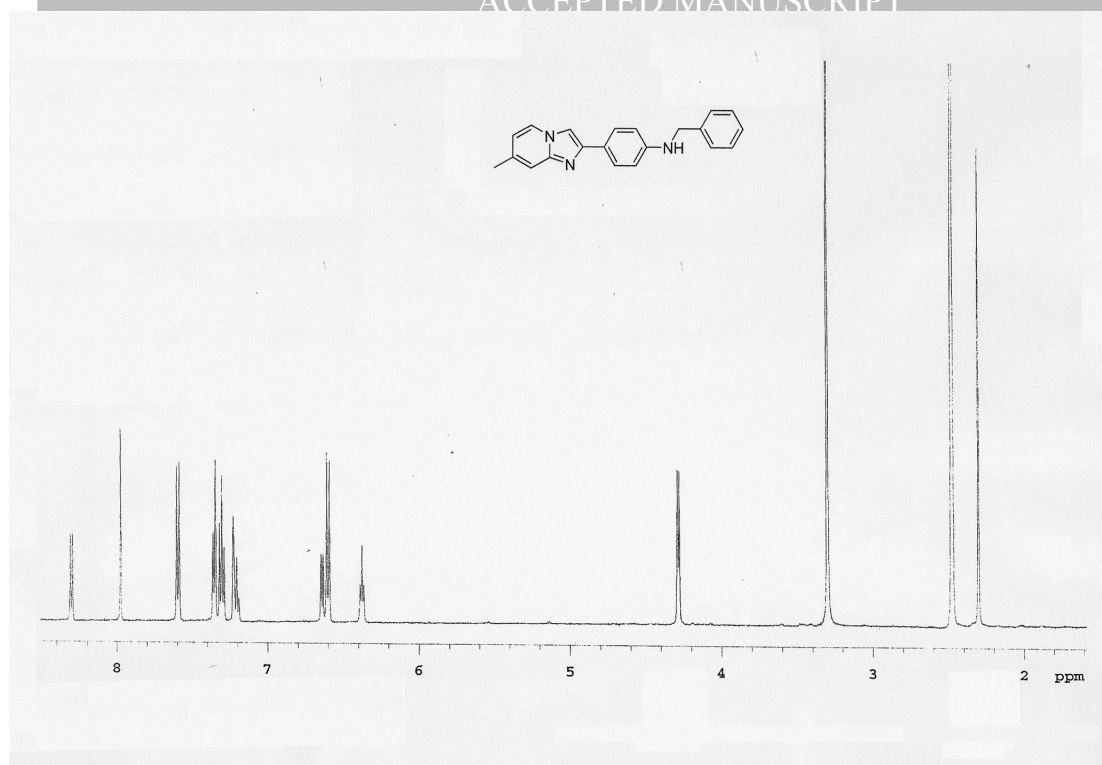
^{13}C NMR (DMSO- d_6) of **2b**.

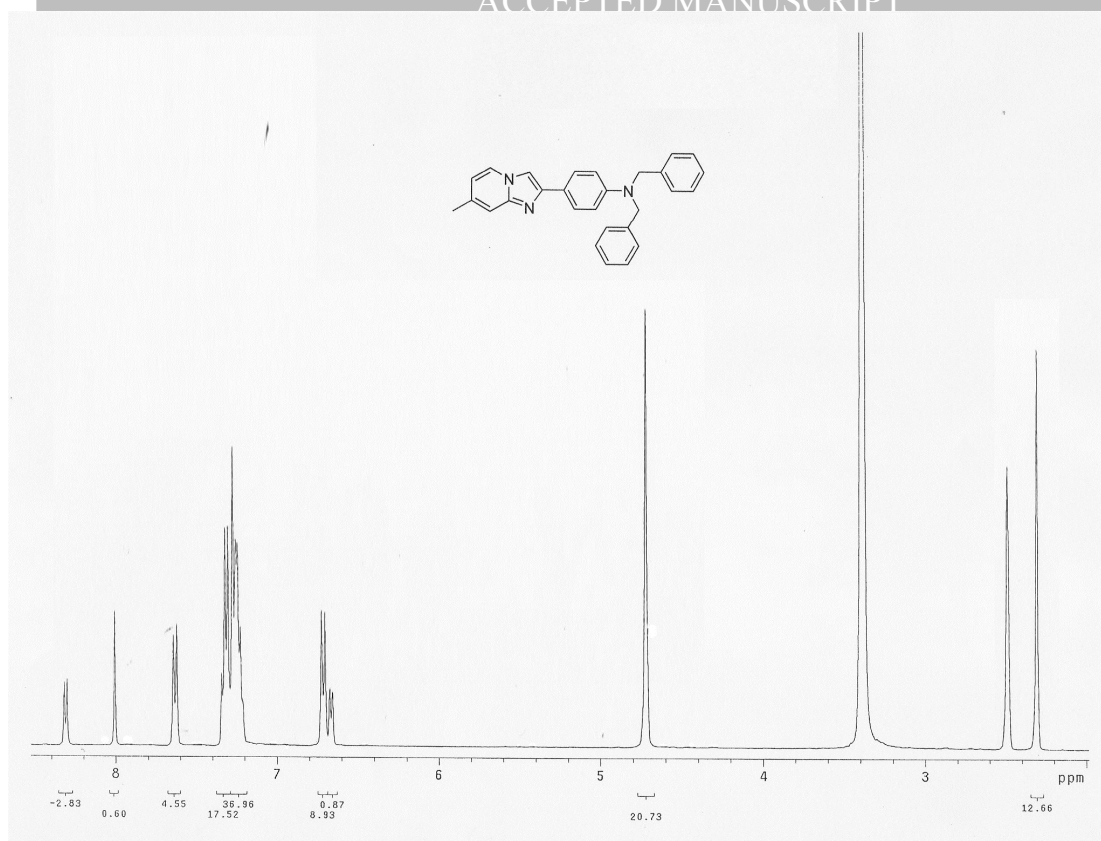




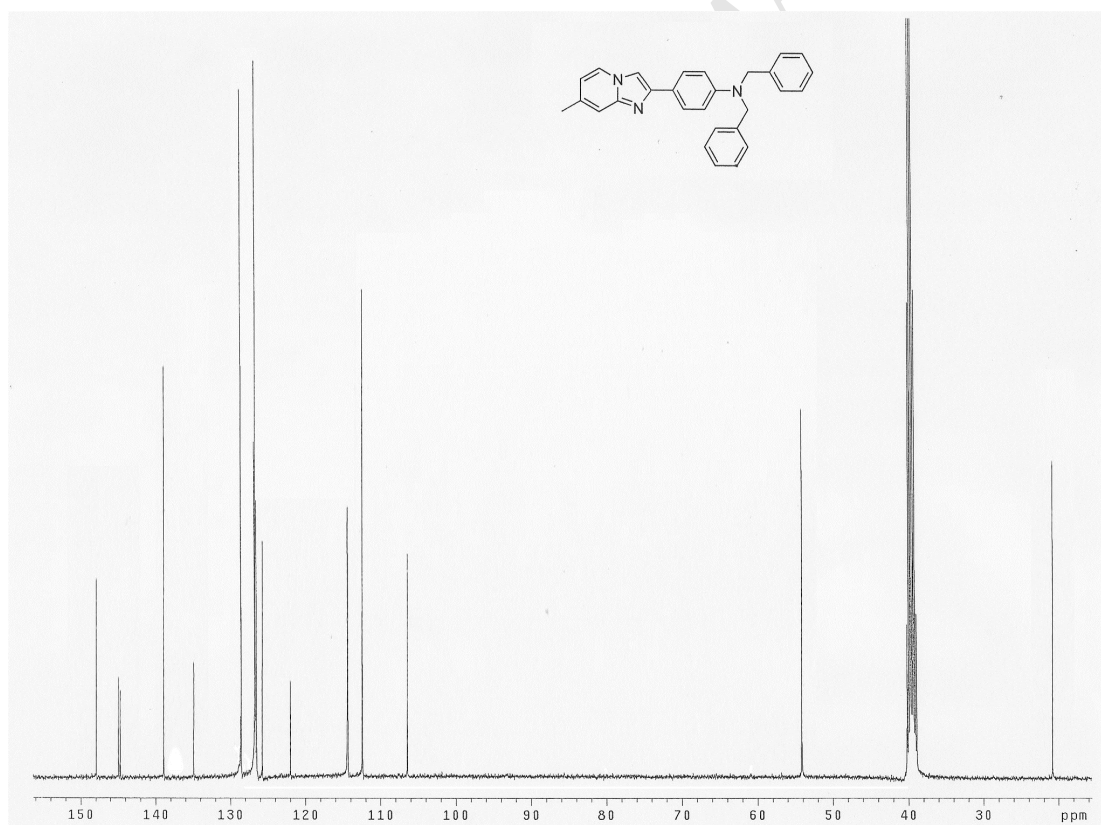








¹H NMR (DMSO-*d*₆) of **4i**.



¹³C NMR (DMSO-*d*₆) of **4i**.